

Localization, Stability, and Resolution of Topological Derivative Based Imaging Functionals in Elasticity *

Habib Ammari [†] Elie Bretin [‡] Josselin Garnier [§] Wenjia Jing [†]
 Hyeonbae Kang [¶] Abdul Wahab ^{||}

December 3, 2024

Abstract

The focus of this work is on rigorous mathematical analysis of the topological derivative based detection algorithms for the localization of an elastic inclusion of vanishing characteristic size. A filtered quadratic misfit is considered and the performance of the topological derivative imaging functional resulting therefrom is analyzed. Our analysis reveals that the imaging functional may not attain its maximum at the location of the inclusion. Moreover, the resolution of the image is below the diffraction limit. Both phenomena are due to the coupling of pressure and shear waves propagating with different wave speeds and polarization directions. A novel imaging functional based on the weighted Helmholtz decomposition of the topological derivative is, therefore, introduced. It is thereby substantiated that the maximum of the imaging functional is attained at the location of the inclusion and the resolution is enhanced and it proves to be the diffraction limit. Finally, we investigate the stability of the proposed imaging functionals with respect to measurement and medium noises.

AMS subject classifications. 35L05, 35R30, 74B05; Secondary 47A52, 65J20

Key words. Elasticity imaging, elastic waves, topological derivative, topological sensitivity, localization, resolution.

1 Introduction

We consider the inverse problem of identifying the location of a small elastic inclusion in a homogeneous isotropic background medium from boundary measurements. The main motivations of this work are Non-Destructive Testing (NDT) of elastic structures for material

*This work was supported by the ERC Advanced Grant Project MULTIMOD–267184 and Korean Ministry of Education, Science, and Technology through grant NRF 2010-0017532.

[†]Department of Mathematics and Applications, Ecole Normale Supérieure, 45 Rue d’Ulm, 75005 Paris, France (habib.ammari@ens.fr, wjing@dma.ens.fr).

[‡]Institut Camille Jordan, INSA de Lyon, 69621, Villeurbanne Cedex, France (elie.bretin@insa-lyon.fr).

[§]Laboratoire de Probabilités et Modèles Aléatoires & Laboratoire Jacques-Louis Lions, Université Paris VII, 75205 Paris Cedex 13, France (garnier@math.jussieu.fr).

[¶]Department of Mathematics, Inha University, Incheon, 402-751, Korea (hbkang@inha.ac.kr).

^{||}Department of Mathematics, COMSATS Institute of Information Technology, 47040, Wah Cantt., Pakistan (wahab@ciitwah.edu.pk).

impurities [13], exploration geophysics [1], and medical diagnosis, in particular, for detection of potential tumors of diminishing size [25].

The long standing problem of anomaly detection has been addressed using a variety of techniques including small volume expansion methods [8, 9], MUSIC type algorithms [4] and time-reversal techniques [3, 6]. The focus of the present study is on the topological derivative based anomaly detection algorithms for elasticity. As shown in [5], in anti-plane elasticity, the topological derivative based imaging functional performs well and is robust with respect to noise and sparse or limited view measurements. The objective of this work is to extend this concept to the general case of linear isotropic elasticity. The analysis is much more delicate in the general case than in the scalar case because of the coupling between the shear and pressure waves.

The concept of topological derivative (TD), initially proposed for shape optimization in [15, 24, 12], has been recently applied to the imaging of small anomalies, see for instance, [13, 14, 17, 18, 19, 20, 23] and references therein. However, its use in the context of imaging has been heuristic and lacks mathematical justifications, notwithstanding its usefulness.

In a prior work [5], acoustic anomaly detection algorithms based on the concept of TD are analyzed and their performance is compared with different detection techniques. Moreover, a stability and resolution analysis is carried out in the presence of measurement and medium noises.

The aim of this work is to analyze the ability of the TD based sensitivity framework for detecting elastic inclusions of vanishing characteristic size. Precisely, our goal is threefold: (i) to perform a rigorous mathematical analysis of the TD based imaging; (2) to design a modified imaging framework based on the analysis. In the case of a density contrast, the modified framework yields a topological derivative based imaging functional, *i.e.*, deriving from the topological derivative of a discrepancy functional. However, in the case where the Lamé coefficients of the small inclusion are different from those of the background medium, the modified functional is rather of a Kirchhoff type. It is based on the correlations between, separately, the shear and compressional parts of the backpropagation of the data and those of the background solution. It can not be derived as the topological derivative of a discrepancy functional; and (3) to investigate the stability of the proposed imaging functionals with respect to measurement and medium noises.

In order to put this work in a proper context, we emphasize some of its significant achievements. A trial inclusion is created in the background medium at a given search location. Then, a discrepancy functional is considered (c.f. Section 3), which is the elastic counterpart of the filtered quadratic misfit proposed in [5]. The search points that minimize the discrepancy between measured data and the fitted data are then sought for. In order to find its minima, the misfit is expanded using the asymptotic expansions due to the perturbation of the displacement field in the presence of an inclusion versus its characteristic size. The first order term in the expansion is then referred to as TD of the misfit (c.f. Section 3.1) which synthesizes its sensitivity relative to the insertion of an inclusion at a given search location. We show that its maximum, which corresponds to the point at which the insertion of the inclusion maximally decreases the misfit, may not be at the location of the true inclusion (c.f. Section 3.2). Further, it is revealed that its resolution is low due to the coupling of pressure and shear wave modes having different wave speeds and polarization directions. Nevertheless, the coupling terms responsible for this degeneracy can be canceled out using a modified imaging framework. A weighed imaging functional is defined using the concept of a weighted Helmholtz decomposition, initially proposed in [3] for time reversal

imaging of extended elastic sources. It is proved that the modified detection algorithm provides a resolution limit of the order of half a wavelength, indeed, as the new functional behaves as the square of the imaginary part of a pressure or shear Green function (c.f. Section 4.2). For simplicity, we restrict ourselves to the study of two particular situations when we have only a density contrast or an elasticity contrast. In order to cater to various applications, we provide explicit results for the canonical cases of circular and spherical inclusions. It is also important to note that the formulae of the TD based functionals are explicit in terms of the incident wave and the free space fundamental solution instead of the Green function in the bounded domain with imposed boundary conditions. This is in contrast with the prior results, see for instance, [18]. Albeit a Neumann boundary condition is imposed on the displacement field, the results of this paper extend to the problem with Dirichlet boundary conditions. A stability analysis of the TD based imaging functionals was also missing in the literature. In this paper we carry out a detailed stability analysis of the proposed imaging functionals with respect to both measurement and medium noises.

The rest of this paper is organized as follows: In Section 2, we introduce some notation and present the asymptotic expansions due to the perturbation of the displacement field in the presence of small inclusions. Section 3 is devoted to the study of TD imaging functional resulting from the expansion of the filtered quadratic misfit with respect to the size of the inclusion. As discussed in Section 3.2, the resolution in TD imaging framework is not optimal. Therefore, a modified imaging framework is established in Section 4. The sensitivity analysis of the modified framework is presented in Section 4.2. Sections 5 and 6 are devoted to the stability analysis with respect to measurement and medium noises, respectively. The paper is concluded in Section 7.

2 Mathematical formulation

This section is devoted to preliminaries, notation and assumptions used in rest of this paper. We also recall a few fundamental results related to small volume asymptotic expansions of the displacement field due to the presence of a penetrable inclusion with respect to the size of the inclusion, which will be essential in the sequel.

2.1 Preliminaries and Notations

Consider a homogeneous isotropic elastic material occupying a bounded domain $\Omega \subset \mathbb{R}^d$, for $d = 2$ or 3 , with connected Lipschitz boundary $\partial\Omega$. Let the Lamé (compressional and shear) parameters of Ω be λ_0 and μ_0 (respectively) in the absence of any inclusion and $\rho_0 > 0$ be the (constant) volume density of the background. Let $D \subset \Omega$ be an elastic inclusion with Lamé parameters λ_1 , μ_1 and density $\rho_1 > 0$. Suppose that D is given by

$$D := \delta B + \mathbf{z}_a \quad (2.1)$$

where B is a bounded Lipschitz domain in \mathbb{R}^d containing the origin and \mathbf{z}_a represents the location of the inclusion D . The small parameter δ represents the characteristic size of the diameter of D . Moreover, we assume that D is separated apart from the boundary $\partial\Omega$, *i.e.*, there exists a constant $c_0 > 0$ such that

$$\inf_{\mathbf{x} \in D} \text{dist}(\mathbf{x}, \partial\Omega) \geq c_0, \quad (2.2)$$

where dist denotes the distance. Further, it is assumed that

$$d\lambda_m + 2\mu_m > 0, \quad \mu_m > 0, \quad m \in \{0, 1\}, \quad (\lambda_0 - \lambda_1)(\mu_0 - \mu_1) \geq 0. \quad (2.3)$$

Consider the following transmission problem with the Neumann boundary condition:

$$\left\{ \begin{array}{ll} \mathcal{L}_{\lambda_0, \mu_0} \mathbf{u} + \rho_0 \omega^2 \mathbf{u} = 0 & \text{in } \Omega \setminus \overline{D}, \\ \mathcal{L}_{\lambda_1, \mu_1} \mathbf{u} + \rho_1 \omega^2 \mathbf{u} = 0 & \text{in } D, \\ \mathbf{u}|_- = \mathbf{u}|_+ & \text{on } \partial D, \\ \frac{\partial \mathbf{u}}{\partial \tilde{\nu}}|_- = \frac{\partial \mathbf{u}}{\partial \nu}|_+ & \text{on } \partial D, \\ \frac{\partial \mathbf{u}}{\partial \nu} = \mathbf{g} & \text{on } \partial \Omega, \end{array} \right. \quad (2.4)$$

where $\omega > 0$ is the angular frequency of the mechanical oscillations, the linear elasticity system $\mathcal{L}_{\lambda_0, \mu_0}$ and the co-normal derivative $\frac{\partial}{\partial \tilde{\nu}}$, associated with parameters (λ_0, μ_0) are defined by

$$\mathcal{L}_{\lambda_0, \mu_0}[\mathbf{w}] := \mu_0 \Delta \mathbf{w} + (\lambda_0 + \mu_0) \nabla \nabla \cdot \mathbf{w} \quad (2.5)$$

and

$$\frac{\partial \mathbf{w}}{\partial \nu} := \lambda_0 (\nabla \cdot \mathbf{w}) \mathbf{n} + \mu_0 (\nabla \mathbf{w}^T + (\nabla \mathbf{w}^T)^T) \mathbf{n}, \quad (2.6)$$

respectively. Here superscript T indicates the transpose of a matrix, \mathbf{n} represents the outward unit normal to ∂D , and $\frac{\partial}{\partial \tilde{\nu}}$ is the co-normal derivative associated with (λ_1, μ_1) . To insure well-posedness, we assume that $\rho_0 \omega^2$ is different from the Neumann eigenvalues of the operator $-\mathcal{L}_{\lambda_0, \mu_0}$ in $(L^2(\Omega))^d$. Using the theory of collectively compact operators (see, for instance, [9, Appendix A.3]), one can show that for small δ the transmission problem (2.4) has a unique solution for any $\mathbf{g} \in (L^2(\partial \Omega))^d$.

Throughout this work, for a domain X , notations $|_-$ and $|_+$ indicate respectively the limits from inside and from outside X to its boundary ∂X , δ_{ij} represents the Kronecker's symbol and

$$\alpha, \beta \in \{P, S\}, \quad i, j, k, l, i', j', k', l', p, q \in \{1, \dots, d\}, \quad m \in \{0, 1\},$$

where P and S stand for pressure and shear parts, respectively.

Statement of the Problem:

The problem under consideration is the following:

Given the displacement field \mathbf{u} , the solution of the Neumann problem (2.4) at the boundary $\partial \Omega$, identify the location \mathbf{z}_a of the inclusion D using a TD based sensitivity framework.

2.2 Asymptotic analysis and fundamental results

Consider the fundamental solution $\mathbf{\Gamma}_m^\omega(\mathbf{x}, \mathbf{y}) := \mathbf{\Gamma}_m^\omega(\mathbf{x} - \mathbf{y})$ of the homogeneous time-harmonic elastic wave equation in \mathbb{R}^d with parameters $(\lambda_m, \mu_m, \rho_m)$, i.e., the solution to

$$(\mathcal{L}_{\lambda_m, \mu_m} + \rho_m \omega^2) \mathbf{\Gamma}_m^\omega(\mathbf{x} - \mathbf{y}) = \delta_{\mathbf{y}}(\mathbf{x}) \mathbf{I}_2, \quad \forall \mathbf{x} \in \mathbb{R}^d, \mathbf{x} \neq \mathbf{y}, \quad (2.7)$$

subject to the *Kupradze's* outgoing radiation conditions [22], where $\delta_{\mathbf{y}}$ is the Dirac mass at \mathbf{y} and \mathbf{I}_2 is the $d \times d$ identity matrix. Let $c_S = \sqrt{\frac{\mu_0}{\rho_0}}$ and $c_P = \sqrt{\frac{\lambda_0 + 2\mu_0}{\rho_0}}$ be the background shear and the pressure wave speeds respectively. Then $\mathbf{\Gamma}_0^\omega$ is given by [1]

$$\mathbf{\Gamma}_0^\omega(\mathbf{x}) = \left\{ \frac{1}{\mu_0} \mathbf{I}_2 G_S^\omega(\mathbf{x}) - \frac{1}{\rho_0 \omega^2} \mathbb{D}_{\mathbf{x}} [G_P^\omega(\mathbf{x}) - G_S^\omega(\mathbf{x})] \right\}, \quad \mathbf{x} \in \mathbb{R}^d, \quad d = 2, 3, \quad (2.8)$$

where the tensor $\mathbb{D}_{\mathbf{x}}$ is defined by

$$\mathbb{D}_{\mathbf{x}} = \nabla_{\mathbf{x}} \otimes \nabla_{\mathbf{x}} = (\partial_{ij})_{i,j=1}^d,$$

and the function G_α^ω is the fundamental solution to the Helmholtz operator, *i.e.*,

$$(\Delta + \kappa_\alpha^2) G_\alpha^\omega(\mathbf{x}) = \delta_{\mathbf{0}}(\mathbf{x}) \quad \mathbf{x} \in \mathbb{R}^d, \mathbf{x} \neq \mathbf{0},$$

subject to the *Sommerfeld's* outgoing radiation condition

$$\left| \frac{\partial G_\alpha^\omega}{\partial \mathbf{n}} - i\kappa_\alpha G_\alpha^\omega \right|(\mathbf{x}) = o(R^{1-d/2}), \quad \mathbf{x} \in \partial B(\mathbf{0}, R),$$

with $B(\mathbf{0}, R)$ being the sphere of radius R and center the origin. Here $\partial_{ij} = \frac{\partial^2}{\partial x_i \partial x_j}$, $\kappa_\alpha := \frac{\omega}{c_\alpha}$ is the wave-number, and $\frac{\partial}{\partial \mathbf{n}}$ represents the normal derivative.

The function G_α^ω is given by

$$G_\alpha^\omega(\mathbf{x}) = \begin{cases} -\frac{i}{4} H_0^{(1)}(\kappa_\alpha |\mathbf{x}|), & d = 2, \\ -\frac{e^{i\kappa_\alpha |\mathbf{x}|}}{4\pi |\mathbf{x}|}, & d = 3, \end{cases} \quad (2.9)$$

where $H_n^{(1)}$ is the order n Hankel function of first kind.

Note that $\mathbf{\Gamma}_0^\omega$ can be decomposed into shear and pressure components *i.e.*

$$\mathbf{\Gamma}_0^\omega(\mathbf{x}) = \mathbf{\Gamma}_{0,S}^\omega(\mathbf{x}) + \mathbf{\Gamma}_{0,P}^\omega(\mathbf{x}), \quad \forall \mathbf{x} \in \mathbb{R}^d, \quad \mathbf{x} \neq \mathbf{0}, \quad (2.10)$$

where

$$\mathbf{\Gamma}_{0,P}^\omega(\mathbf{x}) = -\frac{1}{\mu_0 \kappa_S^2} \mathbb{D}_{\mathbf{x}} G_P^\omega(\mathbf{x}) \quad \text{and} \quad \mathbf{\Gamma}_{0,S}^\omega(\mathbf{x}) = \frac{1}{\mu_0 \kappa_S^2} (\kappa_S^2 \mathbf{I}_2 + \mathbb{D}_{\mathbf{x}}) G_S^\omega(\mathbf{x}). \quad (2.11)$$

Note that $\nabla \cdot \mathbf{\Gamma}_{0,S}^\omega = \mathbf{0}$ and $\nabla \times \mathbf{\Gamma}_{0,P}^\omega = \mathbf{0}$.

Let us define the single layer potential $\mathcal{S}_\Omega^\omega$ associated with $(\mathcal{L}_{\lambda_0, \mu_0} + \rho_0 \omega^2)$ by

$$\mathcal{S}_\Omega^\omega[\Phi](\mathbf{x}) := \int_{\partial\Omega} \mathbf{\Gamma}_0^\omega(\mathbf{x} - \mathbf{y}) \Phi(\mathbf{y}) d\sigma(\mathbf{y}), \quad \mathbf{x} \in \mathbb{R}^d, \quad (2.12)$$

and the boundary integral operator $\mathcal{K}_\Omega^\omega$ by

$$\mathcal{K}_\Omega^\omega[\Phi](\mathbf{x}) := \text{p.v.} \int_{\partial\Omega} \frac{\partial}{\partial \nu_{\mathbf{y}}} \mathbf{\Gamma}_0^\omega(\mathbf{x} - \mathbf{y}) \Phi(\mathbf{y}) d\sigma(\mathbf{y}), \quad \text{a.e. } \mathbf{x} \in \partial\Omega \quad (2.13)$$

for any function $\Phi \in (L^2(\partial\Omega))^d$, where p.v. stands for Cauchy principle value.

Let $(\mathcal{K}_\Omega^\omega)^*$ be the adjoint operator of $\mathcal{K}_\Omega^{-\omega}$ on $(L^2(\partial\Omega))^d$, i.e.,

$$(\mathcal{K}_\Omega^\omega)^*[\Phi](\mathbf{x}) = \text{p.v.} \int_{\partial\Omega} \frac{\partial}{\partial\nu_{\mathbf{x}}} \Gamma_0^\omega(\mathbf{x} - \mathbf{y}) \Phi(\mathbf{y}) d\sigma(\mathbf{y}), \quad \text{a.e. } \mathbf{x} \in \partial\Omega.$$

It is well known, see for instance [2, Section 3.4.3], that the single layer potential, $\mathcal{S}_\Omega^\omega$, enjoys the following jump conditions:

$$\left. \frac{\partial(\mathcal{S}_\Omega^\omega[\Phi])}{\partial\nu} \right|_{\pm}(\mathbf{x}) = \left(\pm \frac{1}{2}I + (\mathcal{K}_\Omega^\omega)^* \right) [\Phi](\mathbf{x}), \quad \text{a.e. } \mathbf{x} \in \partial\Omega. \quad (2.14)$$

Let $\mathbf{N}^\omega(\mathbf{x}, \mathbf{y})$, for all $\mathbf{y} \in \Omega$, be the Neumann solution associated with $(\lambda_0, \mu_0, \rho_0)$ in Ω , i.e.,

$$\begin{cases} (\mathcal{L}_{\lambda_0, \mu_0} + \rho_0 \omega^2) \mathbf{N}^\omega(\mathbf{x}, \mathbf{y}) = -\delta_{\mathbf{y}}(\mathbf{x}) \mathbf{I}_2, & \mathbf{x} \in \Omega, \quad \mathbf{x} \neq \mathbf{y}, \\ \frac{\partial \mathbf{N}^\omega}{\partial\nu}(\mathbf{x}, \mathbf{y}) = 0 & \mathbf{x} \in \partial\Omega. \end{cases} \quad (2.15)$$

Then, by slightly modifying the proof for the case of zero frequency in [8], one can show that the following result holds.

Lemma 2.1. *For all $\mathbf{x} \in \partial\Omega$ and $\mathbf{y} \in \Omega$, we have*

$$\left(-\frac{1}{2}I + \mathcal{K}_\Omega^\omega \right) [\mathbf{N}^\omega(\cdot, \mathbf{y})](\mathbf{x}) = \Gamma_0^\omega(\mathbf{x} - \mathbf{y}). \quad (2.16)$$

For $i, j \in \{1, \dots, d\}$, let \mathbf{v}_{ij} be the solution to

$$\begin{cases} \mathcal{L}_{\lambda_0, \mu_0} \mathbf{v}_{ij} = 0 & \text{in } \mathbb{R}^d \setminus \overline{B}, \\ \mathcal{L}_{\lambda_1, \mu_1} \mathbf{v}_{ij} = 0 & \text{in } B, \\ \mathbf{v}_{ij}|_- = \mathbf{v}_{ij}|_+ & \text{on } \partial B, \\ \frac{\partial \mathbf{v}_{ij}}{\partial \tilde{\nu}}|_- = \frac{\partial \mathbf{v}_{ij}}{\partial \nu}|_+ & \text{on } \partial B, \\ \mathbf{v}_{ij}(\mathbf{x}) - x_i \mathbf{e}_j = O(|\mathbf{x}|^{1-d}) & \text{as } |\mathbf{x}| \rightarrow \infty, \end{cases} \quad (2.17)$$

where $(\mathbf{e}_1, \dots, \mathbf{e}_d)$ denotes the standard basis for \mathbb{R}^d . Then the elastic moment tensor (EMT) $\mathbb{M} := (m_{ijpq})_{i,j,p,q=1}^d$ associated with domain B and the Lamé parameters $(\lambda_0, \mu_0; \lambda_1, \mu_1)$ is defined by

$$m_{ijpq} = \int_{\partial B} \left[\frac{\partial(x_p \mathbf{e}_q)}{\partial \tilde{\nu}} - \frac{\partial(x_p \mathbf{e}_q)}{\partial \nu} \right] \cdot \mathbf{v}_{ij} d\sigma, \quad (2.18)$$

see [8, 11]. In particular, for a circular or a spherical inclusion, \mathbb{M} can be expressed as

$$\mathbb{M} = a \mathbb{I}_4 + b \mathbf{I}_2 \otimes \mathbf{I}_2, \quad (2.19)$$

or equivalently as

$$m_{ijkl} = \frac{a}{2} (\delta_{ik} \delta_{jl} + \delta_{il} \delta_{jk}) + b \delta_{ij} \delta_{kl},$$

for some constants a and b depending only on $\lambda_0, \lambda_1, \mu_0, \mu_1$ and the space dimension d [2, Section 7.3.2]. Here \mathbb{I}_4 is the identity 4-tensor. Note that for any $d \times d$ symmetric matrix \mathbf{A} , $\mathbb{I}_4(\mathbf{A}) = \mathbf{A}$. Furthermore, throughout this paper we make the assumption that $\mu_1 \geq \mu_0$ and $\lambda_1 \geq \lambda_0$ in order to insure that the constants a and b are positive.

It is known that EMT, \mathbb{M} , has the following symmetry property:

$$m_{ijpq} = m_{pqij} = m_{jipq} = m_{ijqp}, \quad (2.20)$$

which allows us to identify \mathbb{M} with a symmetric linear transformation on the space of symmetric $d \times d$ matrices. It also satisfies the positivity property (positive or negative definiteness) on the space of symmetric matrices [8, 11].

Let \mathbf{U} be the background solution associated with $(\lambda_0, \mu_0, \rho_0)$ in Ω , *i.e.*,

$$\begin{cases} (\mathcal{L}_{\lambda_0, \mu_0} + \rho_0 \omega^2) \mathbf{U} = 0, & \text{on } \Omega, \\ \frac{\partial \mathbf{U}}{\partial \nu} = \mathbf{g} & \text{on } \partial\Omega, \end{cases} \quad (2.21)$$

Then, the following result can be obtained using analogous arguments as in [7, 8]; see [4]. Here and throughout this paper

$$\mathbf{A} : \mathbf{B} = \sum_{i,j=1}^d a_{ij} b_{ij}$$

for matrices $\mathbf{A} = (a_{ij})_{i,j=1}^d$ and $\mathbf{B} = (b_{ij})_{i,j=1}^d$.

Theorem 2.2. *Let \mathbf{u} be the solution to (2.4), \mathbf{U} be the background solution defined by (2.21) and $\rho_0 \omega^2$ be different from the Neumann eigenvalues of the operator $-\mathcal{L}_{\lambda_0, \mu_0}$ in $(L^2(\Omega))^d$. Let D be given by (2.1) and the conditions (2.2) and (2.3) are satisfied. Then, for $\omega \delta \ll 1$, the following asymptotic expansion holds uniformly for all $\mathbf{x} \in \partial\Omega$:*

$$\begin{aligned} \mathbf{u}(\mathbf{x}) - \mathbf{U}(\mathbf{x}) = & -\delta^d \left(\nabla \mathbf{U}(\mathbf{z}_a) : \mathbb{M}(B) \nabla_{\mathbf{z}_a} \mathbf{N}^\omega(\mathbf{x}, \mathbf{z}_a) \right. \\ & \left. + \omega^2 (\rho_0 - \rho_1) |B| \mathbf{N}^\omega(\mathbf{x}, \mathbf{z}_a) \mathbf{U}(\mathbf{z}_a) \right) + O(\delta^{d+1}). \end{aligned} \quad (2.22)$$

As a direct consequence of expansion (2.22) and Lemma 2.1, the following result holds.

Corollary 2.3. *Under the assumptions of Theorem 2.2, we have*

$$\begin{aligned} \left(\frac{1}{2} I - \mathcal{K}_\Omega^\omega \right) [\mathbf{u} - \mathbf{U}](\mathbf{x}) = & \delta^d \left(\nabla \mathbf{U}(\mathbf{z}_a) : \mathbb{M}(B) \nabla_{\mathbf{z}_a} \mathbf{\Gamma}_0^\omega(\mathbf{x} - \mathbf{z}_a) \right. \\ & \left. + \omega^2 (\rho_0 - \rho_1) |B| \mathbf{\Gamma}_0^\omega(\mathbf{x} - \mathbf{z}_a) \mathbf{U}(\mathbf{z}_a) \right) + O(\delta^{d+1}) \end{aligned} \quad (2.23)$$

uniformly with respect to $\mathbf{x} \in \partial\Omega$.

Remark 2.4. *We have made use of the following conventions in (2.22) and (2.23):*

$$\left(\nabla \mathbf{U}(\mathbf{z}_a) : \mathbb{M}(B) \nabla_{\mathbf{z}_a} \mathbf{N}^\omega(\mathbf{x}, \mathbf{z}_a) \right)_k = \sum_{i,j=1}^d \left(\partial_i \mathbf{U}_j(\mathbf{z}_a) \sum_{p,q=1}^d m_{ijpq} \partial_p \mathbf{N}_{kq}^\omega(\mathbf{x}, \mathbf{z}_a) \right),$$

and

$$\left(\mathbf{N}^\omega(\mathbf{x}, \mathbf{z}_a) \mathbf{U}(\mathbf{z}_a) \right)_k = \sum_{i=1}^d \mathbf{N}_{ki}^\omega(\mathbf{x}, \mathbf{z}_a) \mathbf{U}_i(\mathbf{z}_a).$$

3 Imaging small inclusions using TD

In this section, we consider a filtered quadratic misfit and introduce a TD based imaging functional resulting therefrom and analyze its performance when identifying true location \mathbf{z}_a of the inclusion D .

For a search point \mathbf{z}^S , let $\mathbf{u}_{\mathbf{z}^S}$ be the solution to (2.4) in the presence of a trial inclusion $D' = \delta' B' + \mathbf{z}^S$ with parameters $(\lambda'_1, \mu'_1, \rho'_1)$, where B' is chosen *a priori* and δ' is small. Assume that

$$d\lambda'_1 + 2\mu'_1 > 0, \quad \mu'_1 > 0, \quad (\lambda_0 - \lambda'_1)(\mu_0 - \mu'_1) \geq 0. \quad (3.1)$$

Consider the elastic counterpart of the filtered quadratic misfit proposed by Ammari *et al.* in [5], that is, the following misfit:

$$\mathcal{E}_f[\mathbf{U}](\mathbf{z}^S) = \frac{1}{2} \int_{\partial\Omega} \left| \left(\frac{1}{2}I - \mathcal{K}_\Omega^\omega \right) [\mathbf{u}_{\mathbf{z}^S} - \mathbf{u}_{\text{meas}}](\mathbf{x}) \right|^2 d\sigma(\mathbf{x}). \quad (3.2)$$

As shown for Helmholtz equations in [5], the identification of the exact location of true inclusion using the classical quadratic misfit

$$\mathcal{E}[\mathbf{U}](\mathbf{z}^S) = \frac{1}{2} \int_{\partial\Omega} |(\mathbf{u}_{\mathbf{z}^S} - \mathbf{u}_{\text{meas}})(\mathbf{x})|^2 d\sigma(\mathbf{x}) \quad (3.3)$$

cannot be guaranteed and the post-processing of the data is necessary. We show in the later part of this section that exact identification can be achieved using filtered quadratic misfit \mathcal{E}_f .

We emphasize that the post-processing compensates for the effects of an imposed Neumann boundary condition on the displacement field.

3.1 Topological derivative of the filtered quadratic misfit

Analogously to Theorem 2.2, the displacement field $\mathbf{u}_{\mathbf{z}^S}$, in the presence of the trial inclusion at the search location, can be expanded as

$$\begin{aligned} \mathbf{u}_{\mathbf{z}^S}(\mathbf{x}) - \mathbf{U}(\mathbf{x}) &= -(\delta')^d \left(\nabla \mathbf{U}(\mathbf{z}^S) : \mathbb{M}'(B') \nabla_{\mathbf{z}^S} \mathbf{N}^\omega(\mathbf{x}, \mathbf{z}^S) \right. \\ &\quad \left. + \omega^2(\rho_0 - \rho'_1) |B'| \mathbf{N}^\omega(\mathbf{x}, \mathbf{z}^S) \mathbf{U}(\mathbf{z}^S) \right) + O((\delta')^{d+1}), \end{aligned} \quad (3.4)$$

for a small $\delta' > 0$, where $\mathbb{M}'(B')$ is the EMT associated with the domain B' and the parameters $(\lambda_0, \mu_0; \lambda'_1, \mu'_1)$. Following the arguments in [5], we obtain, by using Corollary 2.3 and the jump conditions (2.14), that

$$\begin{aligned} \mathcal{E}_f[\mathbf{U}](\mathbf{z}^S) &= \frac{1}{2} \int_{\partial\Omega} \left| \left(\frac{1}{2}I - \mathcal{K}_\Omega^\omega \right) [\mathbf{U} - \mathbf{u}_{\text{meas}}](\mathbf{x}) \right|^2 d\sigma(\mathbf{x}) \\ &\quad + (\delta')^d \Re \left\{ \nabla \mathbf{U}(\mathbf{z}^S) : \mathbb{M}'(B') \nabla \mathbf{w}(\mathbf{z}^S) + \omega^2(\rho_0 - \rho'_1) |B'| \mathbf{U}(\mathbf{z}^S) \cdot \mathbf{w}(\mathbf{z}^S) \right\} \\ &\quad + O((\delta\delta')^d) + O((\delta')^{2d}), \end{aligned} \quad (3.5)$$

where the function \mathbf{w} is defined in terms of the measured data $(\mathbf{U} - \mathbf{u}_{\text{meas}})$ by

$$\mathbf{w}(\mathbf{x}) = \mathcal{S}_\Omega^\omega \left[\left(\frac{1}{2}I - \mathcal{K}_\Omega^\omega \right) [\mathbf{u}_{\text{meas}} - \mathbf{U}] \right](\mathbf{x}), \quad \mathbf{x} \in \Omega. \quad (3.6)$$

The function \mathbf{w} corresponds to backpropagating inside Ω the boundary measurements of $\mathbf{U} - \mathbf{u}_{\text{meas}}$. Substituting (2.23) in (3.6), we find that

$$\begin{aligned} \mathbf{w}(\mathbf{z}^S) &= \delta^d \left(\nabla \overline{\mathbf{U}}(\mathbf{z}_a) : \mathbb{M}(B) \left[\int_{\partial\Omega} \mathbf{\Gamma}_0^\omega(\mathbf{z}^S - \mathbf{x}) \nabla_{\mathbf{z}_a} \overline{\mathbf{\Gamma}}_0^\omega(\mathbf{x} - \mathbf{z}_a) d\sigma(\mathbf{x}) \right] \right. \\ &\quad \left. + \omega^2(\rho_0 - \rho_1)|B| \left[\int_{\partial\Omega} \overline{\mathbf{\Gamma}}_0^\omega(\mathbf{x} - \mathbf{z}_a) \mathbf{\Gamma}_0^\omega(\mathbf{x} - \mathbf{z}^S) d\sigma(\mathbf{x}) \right] \overline{\mathbf{U}}(\mathbf{z}_a) \right) + O(\delta^{d+1}) \end{aligned} \quad (3.7)$$

Definition 3.1. (*Topological derivative of \mathcal{E}_f*) The TD imaging functional associated with \mathcal{E}_f at a search point $\mathbf{z}^S \in \Omega$ is defined by

$$\mathcal{I}_{\text{TD}}[\mathbf{U}](\mathbf{z}^S) := - \frac{\partial \mathcal{E}_f[\mathbf{U}](\mathbf{z}^S)}{\partial (\delta')^d} \Big|_{(\delta')^d=0} \quad (3.8)$$

The functional $\mathcal{I}_{\text{TD}}[\mathbf{U}](\mathbf{z}^S)$ at every search point $\mathbf{z}^S \in \Omega$ synthesizes the sensitivity of the misfit \mathcal{E}_f relative to the insertion of an elastic inclusion $D' = \mathbf{z}^S + \delta' B'$ at that point. The maximum of $\mathcal{I}_{\text{TD}}[\mathbf{U}](\mathbf{z}^S)$ corresponds to the point at which the insertion of an inclusion centered at that point maximally decreases the misfit \mathcal{E}_f . The location of the maximum of $\mathcal{I}_{\text{TD}}[\mathbf{U}](\mathbf{z}^S)$ is, therefore, a good estimate of the location \mathbf{z}_a of the true inclusion, D , that determines the measured field \mathbf{u}_{meas} . Note that from (3.5) it follows that

$$\mathcal{I}_{\text{TD}}[\mathbf{U}](\mathbf{z}^S) = -\Re e \left\{ \nabla \mathbf{U}(\mathbf{z}^S) : \mathbb{M}'(B') \nabla \mathbf{w}(\mathbf{z}^S) + \omega^2(\rho_0 - \rho'_1)|B'| \mathbf{U}(\mathbf{z}^S) \cdot \mathbf{w}(\mathbf{z}^S) \right\} \quad (3.9)$$

where \mathbf{w} is given by (3.7).

3.2 Sensitivity analysis of TD

In this section, we explain why TD imaging functional \mathcal{I}_{TD} may not attain its maximum at the location \mathbf{z}_a of the true inclusion. Notice that the functional \mathcal{I}_{TD} consists of two terms: a density contrast term and an elasticity contrast term with background material. For simplicity and for purely analysis sake, we consider two special cases when we have only the density contrast or the elasticity contrast with reference medium.

3.2.1 Case I: Density contrast

Suppose $\lambda_0 = \lambda_1$ and $\mu_0 = \mu_1$. In this case, the wave function \mathbf{w} satisfies

$$\mathbf{w}(\mathbf{z}^S) \simeq \delta^d \left(\omega^2(\rho_0 - \rho_1)|B| \left[\int_{\partial\Omega} \overline{\mathbf{\Gamma}}_0^\omega(\mathbf{x} - \mathbf{z}_a) \mathbf{\Gamma}_0^\omega(\mathbf{x} - \mathbf{z}^S) d\sigma(\mathbf{x}) \right] \overline{\mathbf{U}}(\mathbf{z}_a) \right). \quad (3.10)$$

Consequently, the imaging functional \mathcal{I}_{TD} at $\mathbf{z}^S \in \Omega$ reduces to

$$\mathcal{I}_{\text{TD}}[\mathbf{U}](\mathbf{z}^S) \simeq C \omega^4 \Re e \left\{ \mathbf{U}(\mathbf{z}^S) \cdot \left[\left(\int_{\partial\Omega} \overline{\mathbf{\Gamma}}_0^\omega(\mathbf{x} - \mathbf{z}_a) \mathbf{\Gamma}_0^\omega(\mathbf{x} - \mathbf{z}^S) d\sigma(\mathbf{x}) \right) \overline{\mathbf{U}}(\mathbf{z}_a) \right] \right\}, \quad (3.11)$$

where

$$C = \delta^d (\rho_0 - \rho'_1)(\rho_0 - \rho_1)|B'| |B|. \quad (3.12)$$

Throughout this paper we assume that

$$(\rho_0 - \rho'_1)(\rho_0 - \rho_1) \geq 0.$$

Let us recall the following estimates from [3, Proposition 2.5], which hold as the distance between the points \mathbf{z}^S and \mathbf{z}_a and the boundary $\partial\Omega$ goes to infinity.

Lemma 3.2. (*Helmholtz - Kirchhoff identities*) For $\mathbf{z}^S, \mathbf{z}_a \in \Omega$ far from the boundary $\partial\Omega$, compared to the wavelength of the wave impinging upon Ω , we have

$$\begin{aligned} \int_{\partial\Omega} \overline{\Gamma_{0,\alpha}^\omega(\mathbf{x} - \mathbf{z}_a)} \Gamma_{0,\alpha}^\omega(\mathbf{x} - \mathbf{z}^S) d\sigma(\mathbf{x}) &\simeq -\frac{1}{c_\alpha \omega} \Im m \{ \Gamma_{0,\alpha}^\omega(\mathbf{z}^S - \mathbf{z}_a) \}, \\ \int_{\partial\Omega} \overline{\Gamma_{0,\alpha}^\omega(\mathbf{x} - \mathbf{z}_a)} \Gamma_{0,\beta}^\omega(\mathbf{x} - \mathbf{z}^S) d\sigma(\mathbf{x}) &\simeq 0, \quad \alpha \neq \beta. \end{aligned}$$

Therefore, by virtue of (2.10) and Lemma 3.2, we can easily get

$$\mathcal{I}_{\text{TD}}[\mathbf{U}](\mathbf{z}^S) \simeq -C \omega^3 \Re e \left\{ \mathbf{U}(\mathbf{z}^S) \cdot \left[\Im m \left\{ \frac{1}{c_P} \Gamma_{0,P}^\omega(\mathbf{z}^S - \mathbf{z}_a) + \frac{1}{c_S} \Gamma_{0,S}^\omega(\mathbf{z}^S - \mathbf{z}_a) \right\} \overline{\mathbf{U}}(\mathbf{z}_a) \right] \right\} \quad (3.13)$$

Let $(\mathbf{e}_{\theta_1}, \mathbf{e}_{\theta_2}, \dots, \mathbf{e}_{\theta_n})$ be n uniformly distributed directions over the unit disk or sphere, and denote by \mathbf{U}_j^P and \mathbf{U}_j^S respectively the plane P - and S -waves, that is,

$$\mathbf{U}_j^P(\mathbf{x}) = e^{i\kappa_P \mathbf{x} \cdot \mathbf{e}_{\theta_j}} \mathbf{e}_{\theta_j} \quad \text{and} \quad \mathbf{U}_j^S(\mathbf{x}) = e^{i\kappa_S \mathbf{x} \cdot \mathbf{e}_{\theta_j}} \mathbf{e}_{\theta_j}^\perp \quad (3.14)$$

for $d = 2$. In three dimensions, we set

$$\mathbf{U}_{j,l}^S(\mathbf{x}) = e^{i\kappa_S \mathbf{x} \cdot \mathbf{e}_{\theta_j}} \mathbf{e}_{\theta_j}^{\perp,l}, \quad l = 1, 2,$$

where $(\mathbf{e}_{\theta_j}, \mathbf{e}_{\theta_j}^{\perp,1}, \mathbf{e}_{\theta_j}^{\perp,2})$ is an orthonormal basis of \mathbb{R}^3 . For ease of notation, in three dimensions, $\mathcal{I}_{\text{TD}}[\mathbf{U}_j^S](\mathbf{z}^S)$ denotes $\sum_{l=1}^2 \mathcal{I}_{\text{TD}}[\mathbf{U}_{j,l}^S](\mathbf{z}^S)$.

We have

$$\frac{1}{n} \sum_{j=1}^n e^{i\kappa_\alpha \mathbf{x} \cdot \mathbf{e}_{\theta_j}} \simeq -4 \left(\frac{\pi}{\kappa_\alpha} \right)^{d-2} \Im m G_\alpha^\omega(\mathbf{x}) \quad (3.15)$$

for large n ; see, for instance, [5]. The following proposition holds.

Proposition 3.3. Let \mathbf{U}_j^α be defined in (3.14), where $j = 1, 2, \dots, n$, for n sufficiently large. Then, for all $\mathbf{z}^S \in \Omega$ far from $\partial\Omega$,

$$\begin{aligned} \frac{1}{n} \sum_{j=1}^n \mathcal{I}_{\text{TD}}[\mathbf{U}_j^P](\mathbf{z}^S) &\simeq 4\mu_0 C \omega^3 \left(\frac{\pi}{\kappa_P} \right)^{d-2} \left(\frac{\kappa_S}{\kappa_P} \right)^2 \left[\frac{1}{c_P} |\Im m \{ \Gamma_{0,P}^\omega(\mathbf{z}^S - \mathbf{z}_a) \}|^2 \right. \\ &\quad \left. + \frac{1}{c_S} \Im m \{ \Gamma_{0,P}^\omega(\mathbf{z}^S - \mathbf{z}_a) \} : \Im m \{ \Gamma_{0,S}^\omega(\mathbf{z}^S - \mathbf{z}_a) \} \right] \quad (3.16) \end{aligned}$$

and

$$\begin{aligned} \frac{1}{n} \sum_{j=1}^n \mathcal{I}_{\text{TD}}[\mathbf{U}_j^S](\mathbf{z}^S) &\simeq 4\mu_0 C \omega^3 \left(\frac{\pi}{\kappa_S} \right)^{d-2} \left[\frac{1}{c_S} |\Im m \{ \Gamma_{0,S}^\omega(\mathbf{z}^S - \mathbf{z}_a) \}|^2 \right. \\ &\quad \left. + \frac{1}{c_P} \Im m \{ \Gamma_{0,P}^\omega(\mathbf{z}^S - \mathbf{z}_a) \} : \Im m \{ \Gamma_{0,S}^\omega(\mathbf{z}^S - \mathbf{z}_a) \} \right] \quad (3.17) \end{aligned}$$

where C is given by (3.12).

Proof. From (3.15) it follows that

$$\begin{aligned} \frac{1}{n} \sum_{j=1}^n e^{i\kappa_P \mathbf{x} \cdot \mathbf{e}_{\theta_j}} \mathbf{e}_{\theta_j} \otimes \mathbf{e}_{\theta_j} &\simeq 4 \left(\frac{\pi}{\kappa_P} \right)^{d-2} \Im m \left\{ \frac{1}{\kappa_P^2} \mathbb{D}_{\mathbf{x}} G_P^\omega(\mathbf{x}) \right\} \\ &\simeq -4\mu_0 \left(\frac{\pi}{\kappa_P} \right)^{d-2} \left(\frac{\kappa_S}{\kappa_P} \right)^2 \Im m \left\{ \mathbf{\Gamma}_{0,P}^\omega(\mathbf{x}) \right\}, \end{aligned} \quad (3.18)$$

and

$$\begin{aligned} \frac{1}{n} \sum_{j=1}^n e^{i\kappa_S \mathbf{x} \cdot \mathbf{e}_{\theta_j}} \mathbf{e}_{\theta_j}^\perp \otimes \mathbf{e}_{\theta_j}^\perp &= \frac{1}{n} \sum_{j=1}^n e^{i\kappa_S \mathbf{x} \cdot \mathbf{e}_{\theta_j}} (\mathbf{I}_2 - \mathbf{e}_{\theta_j} \otimes \mathbf{e}_{\theta_j}) \\ &\simeq -4 \left(\frac{\pi}{\kappa_S} \right)^{d-2} \Im m \left\{ \left(\mathbf{I}_2 + \frac{1}{\kappa_S^2} \mathbb{D}_{\mathbf{x}} \right) G_S^\omega(\mathbf{x}) \right\} \\ &= -4\mu_0 \left(\frac{\pi}{\kappa_S} \right)^{d-2} \Im m \left\{ \mathbf{\Gamma}_{0,S}^\omega(\mathbf{x}) \right\}, \end{aligned} \quad (3.19)$$

where the last equality comes from (2.11). Note that, in three dimensions, (3.19) is to be understood as follows:

$$\frac{1}{n} \sum_{j=1}^n \sum_{l=1}^2 e^{i\kappa_S \mathbf{x} \cdot \mathbf{e}_{\theta_j}} \mathbf{e}_{\theta_j}^{\perp,l} \otimes \mathbf{e}_{\theta_j}^{\perp,l} \simeq -4\mu_0 \left(\frac{\pi}{\kappa_S} \right) \Im m \left\{ \mathbf{\Gamma}_{0,S}^\omega(\mathbf{x}) \right\}. \quad (3.20)$$

Then, using the definition of \mathbf{U}_j^P we compute imaging functional \mathcal{I}_{TD} for n plane P -waves as

$$\begin{aligned} \frac{1}{n} \sum_{j=1}^n \mathcal{I}_{\text{TD}}[\mathbf{U}_j^P](\mathbf{z}^S) &= C\omega^4 \frac{1}{n} \sum_{j=1}^n \Re e \mathbf{U}_j^P(\mathbf{z}^S) \cdot \left[\int_{\partial\Omega} \overline{\mathbf{\Gamma}_0^\omega(\mathbf{x} - \mathbf{z}_a)} \mathbf{\Gamma}_0^\omega(\mathbf{x} - \mathbf{z}^S) d\sigma(\mathbf{x}) \overline{\mathbf{U}_j^P}(\mathbf{z}_a) \right] \\ &\simeq -C\omega^3 \frac{1}{n} \sum_{j=1}^n \Re e e^{i\kappa_P(\mathbf{z}^S - \mathbf{z}_a) \cdot \mathbf{e}_{\theta_j}} \mathbf{e}_{\theta_j} \cdot \left[\Im m \left\{ \frac{1}{c_P} \mathbf{\Gamma}_{0,P}^\omega(\mathbf{z}^S - \mathbf{z}_a) \right. \right. \\ &\quad \left. \left. + \frac{1}{c_S} \mathbf{\Gamma}_{0,S}^\omega(\mathbf{z}^S - \mathbf{z}_a) \right\} \mathbf{e}_{\theta_j} \right] \\ &\simeq -C\omega^3 \Re e \left[\frac{1}{n} \sum_{j=1}^n e^{i\kappa_P(\mathbf{z}^S - \mathbf{z}_a) \cdot \mathbf{e}_{\theta_j}} \mathbf{e}_{\theta_j} \otimes \mathbf{e}_{\theta_j} \right] : \\ &\quad \left[\Im m \left\{ \frac{1}{c_P} \mathbf{\Gamma}_{0,P}^\omega(\mathbf{z}^S - \mathbf{z}_a) + \frac{1}{c_S} \mathbf{\Gamma}_{0,S}^\omega(\mathbf{z}^S - \mathbf{z}_a) \right\} \right]. \end{aligned}$$

Here we used the fact that $\mathbf{e}_{\theta_j} \cdot \mathbf{A} \mathbf{e}_{\theta_j} = \mathbf{e}_{\theta_j} \otimes \mathbf{e}_{\theta_j} : \mathbf{A}$ for a matrix \mathbf{A} , which is easy to check.

Finally, exploiting the approximation (3.18), we conclude that

$$\begin{aligned} \frac{1}{n} \sum_{j=1}^n \mathcal{I}_{\text{TD}}[\mathbf{U}_j^P](\mathbf{z}^S) &\simeq 4\mu_0 C\omega^3 \left(\frac{\pi}{\kappa_P} \right)^{d-2} \left(\frac{\kappa_S}{\kappa_P} \right)^2 \left[\frac{1}{c_P} |\Im m \left\{ \mathbf{\Gamma}_{0,P}^\omega(\mathbf{z}^S - \mathbf{z}_a) \right\}|^2 \right. \\ &\quad \left. + \frac{1}{c_S} \Im m \left\{ \mathbf{\Gamma}_{0,P}^\omega(\mathbf{z}^S - \mathbf{z}_a) \right\} : \Im m \left\{ \mathbf{\Gamma}_{0,S}^\omega(\mathbf{z}^S - \mathbf{z}_a) \right\} \right]. \end{aligned}$$

Similarly, we can compute the imaging functional \mathcal{I}_{TD} for n plane S -waves exploiting the approximation (3.19), as

$$\begin{aligned}
\frac{1}{n} \sum_{j=1}^n \mathcal{I}_{\text{TD}}[\mathbf{U}_j^S](\mathbf{z}^S) &= C\omega^4 \frac{1}{n} \sum_{j=1}^n \Re e \mathbf{U}_j^S(\mathbf{z}^S) \cdot \left[\int_{\partial\Omega} \overline{\mathbf{\Gamma}_0^\omega(\mathbf{x} - \mathbf{z}_a)} \mathbf{\Gamma}_0^\omega(\mathbf{x} - \mathbf{z}^S) d\sigma(\mathbf{x}) \overline{\mathbf{U}_j^S(\mathbf{z}_a)} \right] \\
&\simeq -C\omega^3 \frac{1}{n} \sum_{j=1}^n \Re e e^{i\kappa_S(\mathbf{z}^S - \mathbf{z}_a) \cdot \mathbf{e}_{\theta_j}} \mathbf{e}_{\theta_j}^\perp \cdot \left[\Im m \left\{ \frac{1}{c_P} \mathbf{\Gamma}_{0,P}^\omega(\mathbf{z}^S - \mathbf{z}_a) \right. \right. \\
&\quad \left. \left. + \frac{1}{c_S} \mathbf{\Gamma}_{0,S}^\omega(\mathbf{z}^S - \mathbf{z}_a) \right\} \mathbf{e}_{\theta_j}^\perp \right] \\
&\simeq -C\omega^3 \Re e \left[\frac{1}{n} \sum_{j=1}^n e^{i\kappa_S(\mathbf{z}^S - \mathbf{z}_a) \cdot \mathbf{e}_{\theta_j}} \mathbf{e}_{\theta_j}^\perp \otimes \mathbf{e}_{\theta_j}^\perp \right] : \\
&\quad \left[\Im m \left\{ \frac{1}{c_P} \mathbf{\Gamma}_{0,P}^\omega(\mathbf{z}^S - \mathbf{z}_a) + \frac{1}{c_S} \mathbf{\Gamma}_{0,S}^\omega(\mathbf{z}^S - \mathbf{z}_a) \right\} \right] \\
&\simeq 4\mu_0 C\omega^3 \left(\frac{\pi}{\kappa_S} \right)^{d-2} \left[\frac{1}{c_S} |\Im m \{ \mathbf{\Gamma}_{0,S}^\omega(\mathbf{z}^S - \mathbf{z}_a) \}|^2 \right. \\
&\quad \left. + \frac{1}{c_P} \Im m \{ \mathbf{\Gamma}_{0,P}^\omega(\mathbf{z}^S - \mathbf{z}_a) \} : \Im m \{ \mathbf{\Gamma}_{0,S}^\omega(\mathbf{z}^S - \mathbf{z}_a) \} \right].
\end{aligned}$$

In dimension 3, one should use (3.20) to get the desired result. This completes the proof. \square

From Proposition 3.3, it is not clear that the imaging functional \mathcal{I}_{TD} attains its maximum at \mathbf{z}_a . Moreover, for both $\frac{1}{n} \sum_{j=1}^n \mathcal{I}_{\text{TD}}[\mathbf{U}_j^S](\mathbf{z}^S)$ and $\frac{1}{n} \sum_{j=1}^n \mathcal{I}_{\text{TD}}[\mathbf{U}_j^P](\mathbf{z}^S)$ the resolution at \mathbf{z}_a is not fine enough due to the presence of the term $\Im m \{ \mathbf{\Gamma}_{0,P}^\omega(\mathbf{z}^S - \mathbf{z}_a) \} : \Im m \{ \mathbf{\Gamma}_{0,S}^\omega(\mathbf{z}^S - \mathbf{z}_a) \}$. One way to cancel out this term is to combine $\frac{1}{n} \sum_{j=1}^n \mathcal{I}_{\text{TD}}[\mathbf{U}_j^S](\mathbf{z}^S)$ and $\frac{1}{n} \sum_{j=1}^n \mathcal{I}_{\text{TD}}[\mathbf{U}_j^P](\mathbf{z}^S)$ as follows:

$$\frac{1}{n} \sum_{j=1}^n \left(c_S \left(\frac{\kappa_P}{\pi} \right)^{d-2} \left(\frac{\kappa_P}{\kappa_S} \right)^2 \mathcal{I}_{\text{TD}}[\mathbf{U}_j^P](\mathbf{z}^S) - c_P \left(\frac{\kappa_S}{\pi} \right)^{d-2} \mathcal{I}_{\text{TD}}[\mathbf{U}_j^S](\mathbf{z}^S) \right).$$

However, one arrives at

$$\begin{aligned}
&\frac{1}{n} \sum_{j=1}^n \left(c_S \left(\frac{\kappa_P}{\pi} \right)^{d-2} \left(\frac{\kappa_P}{\kappa_S} \right)^2 \mathcal{I}_{\text{TD}}[\mathbf{U}_j^P](\mathbf{z}^S) - c_P \left(\frac{\kappa_S}{\pi} \right)^{d-2} \mathcal{I}_{\text{TD}}[\mathbf{U}_j^S](\mathbf{z}^S) \right) \\
&\simeq 4\mu_0 C\omega^3 \left(\frac{c_S}{c_P} |\Im m \{ \mathbf{\Gamma}_{0,P}^\omega(\mathbf{z}^S - \mathbf{z}_a) \}|^2 - \frac{c_P}{c_S} |\Im m \{ \mathbf{\Gamma}_{0,S}^\omega(\mathbf{z}^S - \mathbf{z}_a) \}|^2 \right),
\end{aligned}$$

which is not a sum of positive terms and then can not guarantee that the maximum of the obtained imaging functional is at the location of the inclusion.

3.2.2 Case II: Elasticity contrast

Suppose $\rho_0 = \rho_1$. Further, we assume for simplicity that $\mathbb{M} = \mathbb{M}'(B') = \mathbb{M}(B)$. From Lemma 3.2 we have

$$\begin{aligned} \int_{\partial\Omega} \nabla_{\mathbf{z}_a} \overline{\Gamma_0^\omega}(\mathbf{x} - \mathbf{z}_a) \nabla_{\mathbf{z}^S} \Gamma_0^\omega(\mathbf{x} - \mathbf{z}^S) d\sigma(\mathbf{x}) &\simeq -\frac{1}{c_S \omega} \Im m \left\{ \nabla_{\mathbf{z}_a} \nabla_{\mathbf{z}^S} \Gamma_{0,S}^\omega(\mathbf{z}^S - \mathbf{z}_a) \right\} \\ &\quad - \frac{1}{c_P \omega} \Im m \left\{ \nabla_{\mathbf{z}_a} \nabla_{\mathbf{z}^S} \Gamma_{0,P}^\omega(\mathbf{z}^S - \mathbf{z}_a) \right\}. \end{aligned} \quad (3.21)$$

Then, using (3.7) and (3.21), $\mathcal{I}_{\text{TD}}[\mathbf{U}](\mathbf{z}^S)$ at $\mathbf{z}^S \in \Omega$ becomes

$$\begin{aligned} \mathcal{I}_{\text{TD}}[\mathbf{U}](\mathbf{z}^S) &= -\delta^d \Re e \nabla \mathbf{U}(\mathbf{z}^S) : \mathbb{M} \nabla \mathbf{w}(\mathbf{z}^S) \\ &= \delta^d \Re e \nabla \mathbf{U}(\mathbf{z}^S) : \mathbb{M} \left[\int_{\partial\Omega} \nabla_{\mathbf{z}_a} \overline{\Gamma_0^\omega}(\mathbf{x} - \mathbf{z}_a) \nabla_{\mathbf{z}^S} \Gamma_0^\omega(\mathbf{x} - \mathbf{z}^S) d\sigma(\mathbf{x}) : \mathbb{M} \overline{\nabla \mathbf{U}}(\mathbf{z}_a) \right] \\ &\simeq \frac{\delta^d}{\omega} \Re e \nabla \mathbf{U}(\mathbf{z}^S) : \mathbb{M} \left[\nabla^2 \left(\Im m \left\{ \widetilde{\Gamma_0^\omega}(\mathbf{z}^S - \mathbf{z}_a) \right\} \right) : \mathbb{M} \overline{\nabla \mathbf{U}}(\mathbf{z}_a) \right], \end{aligned} \quad (3.22)$$

where

$$\widetilde{\Gamma_0^\omega}(\mathbf{z}^S - \mathbf{z}_a) = \frac{1}{c_P} \Gamma_{0,P}^\omega(\mathbf{z}^S - \mathbf{z}_a) + \frac{1}{c_S} \Gamma_{0,S}^\omega(\mathbf{z}^S - \mathbf{z}_a). \quad (3.23)$$

Let us define

$$J_{\alpha,\beta}(\mathbf{z}^S) := \left(\mathbb{M} \Im m \left[(\nabla^2 \Gamma_{0,\alpha}^\omega)(\mathbf{z}^S - \mathbf{z}_a) \right] \right) : \left(\mathbb{M} \Im m \left[(\nabla^2 \Gamma_{0,\beta}^\omega)(\mathbf{z}^S - \mathbf{z}_a) \right] \right)^T, \quad (3.24)$$

where $\mathbb{A}^T = (A_{kl ij})$ if \mathbb{A} is the 4-tensor given by $\mathbb{A} = (A_{ijkl})$. Here $\mathbb{A} : \mathbb{B} = \sum_{ijkl} A_{ijkl} B_{ijkl}$ for any 4-tensors $\mathbb{A} = (A_{ijkl})$ and $\mathbb{B} = (B_{ijkl})$.

The following result holds.

Proposition 3.4. *Let \mathbf{U}_j^α be defined in (3.14), where $j = 1, 2, \dots, n$, for n sufficiently large. Let $J_{\alpha,\beta}$ be defined by (3.24). Then, for all $\mathbf{z}^S \in \Omega$ far from $\partial\Omega$,*

$$\frac{1}{n} \sum_{j=1}^n \mathcal{I}_{\text{TD}}[\mathbf{U}_j^P](\mathbf{z}^S) \simeq 4\delta^d \frac{\mu_0}{\omega} \left(\frac{\pi}{\kappa_P} \right)^{d-2} \left(\frac{\kappa_S}{\kappa_P} \right)^2 \left(\frac{1}{c_P} J_{P,P}(\mathbf{z}^S) + \frac{1}{c_S} J_{S,P}(\mathbf{z}^S) \right) \quad (3.25)$$

and

$$\frac{1}{n} \sum_{j=1}^n \mathcal{I}_{\text{TD}}[\mathbf{U}_j^S](\mathbf{z}^S) \simeq 4\delta^d \frac{\mu_0}{\omega} \left(\frac{\pi}{\kappa_S} \right)^{d-2} \left(\frac{1}{c_S} J_{S,S}(\mathbf{z}^S) + \frac{1}{c_P} J_{S,P}(\mathbf{z}^S) \right). \quad (3.26)$$

Proof. Let us compute \mathcal{I}_{TD} for n plane P -waves, i.e.

$$\begin{aligned} \frac{1}{n} \sum_{j=1}^n \mathcal{I}_{\text{TD}}[\mathbf{U}_j^P](\mathbf{z}^S) &= \frac{\delta^d}{\omega} \frac{1}{n} \Re e \sum_{j=1}^n \nabla \mathbf{U}_j^P(\mathbf{z}^S) : \mathbb{M} \left[\Im m \left\{ (\nabla^2 \widetilde{\Gamma_0^\omega})(\mathbf{z}^S - \mathbf{z}_a) \right\} : \mathbb{M} \overline{\nabla \mathbf{U}_j^P}(\mathbf{z}_a) \right] \\ &\simeq \delta^d \frac{\omega}{c_P^2} \frac{1}{n} \Re e \sum_{j=1}^n e^{i\kappa_P(\mathbf{z}^S - \mathbf{z}_a) \cdot \mathbf{e}_{\theta_j}} \mathbf{e}_{\theta_j} \otimes \mathbf{e}_{\theta_j} : \\ &\quad \mathbb{M} \left(\Im m \left\{ \nabla^2 \widetilde{\Gamma_0^\omega}(\mathbf{z}^S - \mathbf{z}_a) \right\} : \mathbb{M} \mathbf{e}_{\theta_j} \otimes \mathbf{e}_{\theta_j} \right). \end{aligned} \quad (3.27)$$

Equivalently,

$$\begin{aligned} \frac{1}{n} \sum_{j=1}^n \mathcal{I}_{\text{TD}}[\mathbf{U}_j^P](\mathbf{z}^S) &= \delta^d \frac{\omega}{c_P^2} \frac{1}{n} \Re e \sum_{j=1}^n e^{i\kappa_P(\mathbf{z}^S - \mathbf{z}_a) \cdot \mathbf{e}_{\theta_j}} \sum_{i,k,l,m=1}^d \sum_{i',k',l',m'=1}^d A_{ik}^{\theta_j} m_{lmik} \\ &\quad \times \Im m \left\{ \left((\partial_{li'}^2 \widetilde{\Gamma}_0^\omega)(\mathbf{z}^S - \mathbf{z}_a) \right)_{mk'} \right\} m_{l'm'i'k'} A_{l'm'}^{\theta_j} \end{aligned} \quad (3.28)$$

where the matrix $\mathbf{A}^{\theta_j} = (A_{ik}^{\theta_j})_{ik}$ is defined as $\mathbf{A}^{\theta_j} := \mathbf{e}_{\theta_j} \otimes \mathbf{e}_{\theta_j}$. It follows that

$$\begin{aligned} \frac{1}{n} \sum_{j=1}^n \mathcal{I}_{\text{TD}}[\mathbf{U}_j^P](\mathbf{z}^S) &= \delta^d \Re e \sum_{i,k,l,m=1}^d \sum_{i',k',l',m'=1}^d m_{lmik} m_{l'm'i'k'} \Im m \left[\left((\partial_{li'}^2 \widetilde{\Gamma}_0^\omega)(\mathbf{z}^S - \mathbf{z}_a) \right)_{mk'} \right] \\ &\quad \times \left(\frac{\omega}{c_P^2} \frac{1}{n} \sum_{j=1}^n e^{i\kappa_P(\mathbf{z}^S - \mathbf{z}_a) \cdot \mathbf{e}_{\theta_j}} A_{ik}^{\theta_j} A_{l'm'}^{\theta_j} \right). \end{aligned} \quad (3.29)$$

Recall that for n sufficiently large, we have from (3.18)

$$\frac{1}{n} \sum_{j=1}^n e^{i\kappa_P \mathbf{x} \cdot \mathbf{e}_{\theta_j}} \mathbf{e}_{\theta_j} \otimes \mathbf{e}_{\theta_j} \simeq -4\mu_0 \left(\frac{\pi}{\kappa_P} \right)^{d-2} \left(\frac{\kappa_S}{\kappa_P} \right)^2 \Im m \{ \Gamma_{0,P}^\omega(\mathbf{x}) \}$$

(with the version (3.20) in dimension 3). Taking the Hessian of the previous approximation leads to

$$\begin{aligned} \frac{1}{n} \sum_{j=1}^n e^{i\kappa_P \mathbf{x} \cdot \mathbf{e}_{\theta_j}} \mathbf{e}_{\theta_j} \otimes \mathbf{e}_{\theta_j} \otimes \mathbf{e}_{\theta_j} \otimes \mathbf{e}_{\theta_j} &\simeq 4\mu_0 \frac{c_P^2}{\omega^2} \left(\frac{\pi}{\kappa_P} \right)^{d-2} \left(\frac{\kappa_S}{\kappa_P} \right)^2 \Im m \{ \nabla^2 \Gamma_{0,P}^\omega(\mathbf{x}) \} \\ &\simeq 4\mu_0 \frac{c_P^4}{\omega^2 c_S^2} \left(\frac{\pi}{\kappa_P} \right)^{d-2} \Im m \{ \nabla^2 \Gamma_{0,P}^\omega(\mathbf{x}) \}. \end{aligned} \quad (3.30)$$

Then, by virtue of (3.18) and (3.30), we obtain

$$\begin{aligned} \frac{1}{n} \sum_{j=1}^n \mathcal{I}_{\text{TD}}[\mathbf{U}_j^P](\mathbf{z}^S) &\simeq \delta^d \frac{4\mu_0}{\omega} \left(\frac{\pi}{\kappa_P} \right)^{d-2} \left(\frac{\kappa_S}{\kappa_P} \right)^2 \sum_{i,k,l,m=1}^d \sum_{i',k',l',m'=1}^d m_{lmik} m_{l'm'i'k'} \\ &\quad \times \Im m \left\{ \left((\partial_{li'}^2 \widetilde{\Gamma}_0^\omega)(\mathbf{z}^S - \mathbf{z}_a) \right)_{mk'} \right\} \Im m \left\{ \left((\partial_{l'i}^2 \Gamma_{0,P}^\omega)(\mathbf{z}^S - \mathbf{z}_a) \right)_{m'k} \right\} \\ &\simeq \delta^d \frac{4\mu_0}{\omega} \left(\frac{\pi}{\kappa_P} \right)^{d-2} \left(\frac{\kappa_S}{\kappa_P} \right)^2 \sum_{i,k,i',k'=1}^d \left(\sum_{l,m=1}^d m_{lmik} \Im m \left\{ \left((\partial_{li'}^2 \widetilde{\Gamma}_0^\omega)(\mathbf{z}^S - \mathbf{z}_a) \right)_{mk'} \right\} \right) \\ &\quad \times \left(\sum_{l',m'=1}^d m_{l'm'i'k'} \Im m \left\{ \left((\partial_{l'i}^2 \Gamma_{0,P}^\omega)(\mathbf{z}^S - \mathbf{z}_a) \right)_{m'k} \right\} \right). \end{aligned}$$

Therefore, by the definition (3.24) of $J_{\alpha,\beta}$, we conclude that

$$\begin{aligned} \frac{1}{n} \sum_{j=1}^n \mathcal{I}_{\text{TD}}[\mathbf{U}_j^P](\mathbf{z}^S) &\simeq \delta^d \frac{4\mu_0}{\omega} \left(\frac{\pi}{\kappa_P}\right)^{d-2} \left(\frac{\kappa_S}{\kappa_P}\right)^2 \left(\mathbb{M} \Im m \left\{ \nabla^2 \widetilde{\Gamma}_0^\omega(\mathbf{z}^S - \mathbf{z}_a) \right\} \right) \\ &\quad : \left(\mathbb{M} \Im m \left\{ \nabla^2 \Gamma_{0,P}^\omega(\mathbf{z}^S - \mathbf{z}_a) \right\} \right)^T \\ &\simeq \delta^d \frac{4\mu_0}{\omega} \left(\frac{\pi}{\kappa_P}\right)^{d-2} \left(\frac{\kappa_S}{\kappa_P}\right)^2 \left(\frac{1}{c_P} J_{P,P}(\mathbf{z}^S) + \frac{1}{c_S} J_{S,P}(\mathbf{z}^S) \right). \end{aligned}$$

Similarly, consider the case of plane S -waves and compute \mathcal{I}_{TD} for n directions. We have

$$\begin{aligned} \frac{1}{n} \sum_{j=1}^n \mathcal{I}_{\text{TD}}[\mathbf{U}_j^S](\mathbf{z}^S) &= \frac{\delta^d}{\omega} \frac{1}{n} \Re e \sum_{j=1}^n \nabla \mathbf{U}_j^S(\mathbf{z}^S) : \mathbb{M} \left(\Im m \left\{ (\nabla^2 \widetilde{\Gamma}_0^\omega)(\mathbf{z}^S - \mathbf{z}_a) \right\} : \mathbb{M} \overline{\nabla \mathbf{U}_j^S}(\mathbf{z}_a) \right) \\ &\simeq \delta^d \frac{\omega}{c_S^2} \frac{1}{n} \Re e \sum_{j=1}^n e^{i\kappa_S(\mathbf{z}^S - \mathbf{z}_a) \cdot \mathbf{e}_{\theta_j}} \mathbf{e}_{\theta_j}^\perp \otimes \mathbf{e}_{\theta_j} : \mathbb{M} \\ &\quad \left(\Im m \left\{ (\nabla^2 \widetilde{\Gamma}_0^\omega)(\mathbf{z}^S - \mathbf{z}_a) \right\} : \mathbb{M} \mathbf{e}_{\theta_j}^\perp \otimes \mathbf{e}_{\theta_j} \right) \\ &\simeq \delta^d \frac{\omega}{c_S^2} \frac{1}{n} \Re e \sum_{j=1}^n e^{i\kappa_S(\mathbf{z}^S - \mathbf{z}_a) \cdot \mathbf{e}_{\theta_j}} \sum_{i,k,l,m=1}^d \sum_{i',k',l',m'=1}^d B_{ik}^{\theta_j} m_{lmik} \\ &\quad \times \Im m \left\{ \left((\partial_{li'}^2 \widetilde{\Gamma}_0^\omega)(\mathbf{z}^S - \mathbf{z}_a) \right)_{mk'} \right\} m_{l'm'i'k'} B_{l'm'}^{\theta_j} \quad (3.31) \end{aligned}$$

where the matrix $\mathbf{B}^{\theta_j} = (B_{ik}^{\theta_j})_{ik}$ is defined as $\mathbf{B}^{\theta_j} = \mathbf{e}_{\theta_j} \otimes \mathbf{e}_{\theta_j}^\perp$. It follows that

$$\begin{aligned} \frac{1}{n} \sum_{j=1}^n \mathcal{I}_{\text{TD}}[\mathbf{U}_j^S](\mathbf{z}^S) &= \delta^d \sum_{i,k,l,m=1}^d \sum_{i',k',l',m'=1}^d m_{lmik} m_{l'm'i'k'} \Im m \left[\partial_{li'}^2 \left(\widetilde{\Gamma}_0^\omega(\mathbf{z}^S - \mathbf{z}_a) \right)_{mk'} \right] \\ &\quad \left(\frac{\omega}{c_S^2} \frac{1}{n} \sum_{j=1}^n e^{i\kappa_S(\mathbf{z}^S - \mathbf{z}_a) \cdot \mathbf{e}_{\theta_j}} B_{ik}^{\theta_j} B_{l'm'}^{\theta_j} \right). \quad (3.32) \end{aligned}$$

Now, recall from (3.19) that for n sufficiently large, we have

$$\frac{1}{n} \sum_{j=1}^n e^{i\kappa_S \mathbf{x} \cdot \mathbf{e}_{\theta_j}} \mathbf{e}_{\theta_j}^\perp \otimes \mathbf{e}_{\theta_j}^\perp \simeq -4\mu_0 \left(\frac{\pi}{\kappa_S}\right)^{d-2} \Im m \left\{ \Gamma_{0,S}^\omega(\mathbf{x}) \right\}.$$

Taking the Hessian of this approximation leads to

$$\frac{1}{n} \sum_{j=1}^n e^{i\kappa_S \mathbf{x} \cdot \mathbf{e}_{\theta_j}} \mathbf{e}_{\theta_j} \otimes \mathbf{e}_{\theta_j}^\perp \otimes \mathbf{e}_{\theta_j} \otimes \mathbf{e}_{\theta_j}^\perp \simeq 4\mu_0 \frac{c_S^2}{\omega^2} \left(\frac{\pi}{\kappa_S}\right)^{d-2} \Im m \left\{ \nabla^2 \Gamma_{0,S}^\omega(\mathbf{x}) \right\}, \quad (3.33)$$

where we have made use of the convention

$$(\nabla^2 \Gamma_{0,S}^\omega)_{ijkl} = \partial_{ik} (\Gamma_{0,S}^\omega)_{jl}.$$

Then, by using (3.19), (3.33) and the similar arguments as in the case of P -waves, we arrive at

$$\begin{aligned}
\frac{1}{n} \sum_{j=1}^n \mathcal{I}_{\text{TD}}[\mathbf{U}_j^S](\mathbf{z}^S) &\simeq \delta^d \frac{4\mu_0}{\omega} \left(\frac{\pi}{\kappa_S}\right)^{d-2} \sum_{i,k,l,m=1}^d \sum_{i',k',l',m'=1}^d m_{lmik} m_{l'm'i'k'} \\
&\quad \times \Im m \left\{ \left((\partial_{li'}^2 \widetilde{\mathbf{\Gamma}}_0^\omega) \right)_{mk'} (\mathbf{z}^S - \mathbf{z}_a) \right\} \\
&\quad \times \Im m \left\{ \left((\partial_{l'i}^2 \mathbf{\Gamma}_{0,S}^\omega) \right)_{m'k} (\mathbf{z}^S - \mathbf{z}_a) \right\} \\
&\simeq \delta^d \frac{4\mu_0}{\omega} \left(\frac{\pi}{\kappa_S}\right)^{d-2} \left(\mathbb{M} \Im m \left\{ (\nabla^2 \widetilde{\mathbf{\Gamma}}_0^\omega)(\mathbf{z}^S - \mathbf{z}_a) \right\} \right) : \\
&\quad \left(\mathbb{M} \Im m \left\{ (\nabla^2 \mathbf{\Gamma}_{0,S}^\omega)(\mathbf{z}^S - \mathbf{z}_a) \right\} \right)^T \\
&\simeq \delta^d \frac{4\mu_0}{\omega} \left(\frac{\pi}{\kappa_S}\right)^{d-2} \left(\frac{1}{c_P} J_{P,S}(\mathbf{z}^S) + \frac{1}{c_S} J_{S,S}(\mathbf{z}^S) \right).
\end{aligned}$$

This completes the proof. \square

As observed in Section 3.2.1, Proposition 3.4 shows that the resolution of \mathcal{I}_{TD} deteriorates due to the presence of the coupling term

$$J_{P,S}(\mathbf{z}^S) = \left(\mathbb{M} \Im m \left\{ (\nabla^2 \mathbf{\Gamma}_{0,S}^\omega)(\mathbf{z}^S - \mathbf{z}_a) \right\} \right) : \left(\mathbb{M} \Im m \left\{ (\nabla^2 \mathbf{\Gamma}_{0,P}^\omega)(\mathbf{z}^S - \mathbf{z}_a) \right\} \right)^T. \quad (3.34)$$

3.2.3 Summary

To conclude, we summarize the results of this section below.

- Propositions 3.3 and 3.4 indicate that the imaging function \mathcal{I}_{TD} may not attain its maximum at the true location, \mathbf{z}_a , of the inclusion D .
- In both cases, the resolution of the localization of elastic anomaly D degenerates due to the presence of the coupling terms $\Im m \left\{ \mathbf{\Gamma}_{0,P}^\omega(\mathbf{z}^S - \mathbf{z}_a) \right\} : \Im m \left\{ \mathbf{\Gamma}_{0,S}^\omega(\mathbf{z}^S - \mathbf{z}_a) \right\}$ and $J_{P,S}(\mathbf{z}^S)$, respectively.
- In order to enhance imaging resolution to its optimum and insure that the imaging functional attains its maximum only at the location of the inclusion, one must eradicate the coupling terms.

4 Modified imaging framework

In this section, in order to achieve a better localization and resolution properties, we introduce a modified imaging framework based on a weighted Helmholtz decomposition of the TD imaging functional. We will show that the modified framework leads to both a better localization (in the sense that the modified imaging functional attains its maximum at the location of the inclusion) and a better resolution than the classical TD based sensitivity framework. It is worthwhile mentioning that the classical framework performs quite well

for the case of Helmholtz equation [5] and the resolution and localization deteriorations are purely dependent on the elastic nature of the problem, that is, due to the coupling of pressure and shear waves propagating with different wave speeds and polarization directions.

It should be noted that in the case of a density contrast only, the modified imaging functional is still a topological derivative based one, *i.e.*, obtained as the topological derivative of a discrepancy functional. This holds because of the nonconversion of waves (from shear to compressional and vice versa) in the presence of only a small inclusion with a contrast density. However, in the presence of a small inclusion with different Lamé coefficients with the background medium, there is a mode conversion; see, for instance, [21]. As a consequence, the modified functional proposed here can not be written in such a case as the topological derivative of a discrepancy functional. It is rather a Kirchhoff-type imaging functional.

4.1 Weighted imaging functional

Following [3], we introduce a weighted topological derivative imaging functional \mathcal{I}_W , and justify that it provides a better localization of the inclusion D than \mathcal{I}_{TD} . This new functional \mathcal{I}_W can be seen as a correction based on a weighted Helmholtz decomposition of \mathcal{I}_{TD} . In fact, using the standard L^2 -theory of the Helmholtz decomposition (see, for instance, [16]), we find that in the search domain the pressure and the shear components of \mathbf{w} , defined by (3.6), can be written as

$$\mathbf{w} = \nabla \times \psi_{\mathbf{w}} + \nabla \phi_{\mathbf{w}}. \quad (4.1)$$

We define respectively the Helmholtz decomposition operators \mathcal{H}^P and \mathcal{H}^S by

$$\mathcal{H}^P[\mathbf{w}] := \nabla \phi_{\mathbf{w}} \quad \text{and} \quad \mathcal{H}^S[\mathbf{w}] := \nabla \times \psi_{\mathbf{w}}. \quad (4.2)$$

Actually, the decomposition $\mathbf{w} = \mathcal{H}^P[\mathbf{w}] + \mathcal{H}^S[\mathbf{w}]$ can be found by solving a Neumann problem in the search domain [16]. Then we multiply the components of \mathbf{w} with c_P and c_S , the background pressure and the shear wave speeds respectively. Finally, we define \mathcal{I}_W by

$$\begin{aligned} \mathcal{I}_W[\mathbf{U}] &= c_P \Re \left\{ -\nabla \mathcal{H}^P[\mathbf{U}] : \mathbb{M}'(B') \nabla \mathcal{H}^P[\mathbf{w}] + \omega^2 \left(\frac{\rho'_1}{\rho_0} - 1 \right) |B'| \mathcal{H}^P[\mathbf{U}] \cdot \mathcal{H}^P[\mathbf{w}] \right\} \\ &+ c_S \Re \left\{ -\nabla \mathcal{H}^S[\mathbf{U}] : \mathbb{M}'(B') \nabla \mathcal{H}^S[\mathbf{w}] + \omega^2 \left(\frac{\rho'_1}{\rho_0} - 1 \right) |B'| \mathcal{H}^S[\mathbf{U}] \cdot \mathcal{H}^S[\mathbf{w}] \right\} \end{aligned} \quad (4.3)$$

We rigorously explain in the next section why this new functional should be better than imaging functional \mathcal{I}_{TD} .

4.2 Sensitivity analysis of weighted imaging functional

In this section, we explain why imaging functional \mathcal{I}_W attains its maximum at the location \mathbf{z}_a of the true inclusion with a better resolution than \mathcal{I}_{TD} . In fact, as shown in the later part of this section, \mathcal{I}_W behaves like the square of the imaginary part of a pressure or a shear Green function depending upon the incident wave. Consequently, it provides a resolution of the order of half a wavelength. For simplicity, we once again consider special cases of only density contrast and only elasticity contrast.

4.2.1 Case I: Density contrast

Suppose $\lambda_0 = \lambda_1$ and $\mu_0 = \mu_1$. Recall that in this case, the wave function \mathbf{w} is given by (3.10). Note that $\mathcal{H}^\alpha[\mathbf{\Gamma}_0^\omega] = \mathbf{\Gamma}_{0,\alpha}^\omega, \alpha \in \{P, S\}$. Therefore, the imaging functional \mathcal{I}_W at $\mathbf{z}^S \in \Omega$ turns out to be

$$\begin{aligned} \mathcal{I}_W[\mathbf{U}](\mathbf{z}^S) &= C\omega^4 \Re e \left(c_P \mathcal{H}^P[\mathbf{U}](\mathbf{z}^S) \cdot \left[\left(\int_{\partial\Omega} \overline{\mathbf{\Gamma}_0^\omega}(\mathbf{x} - \mathbf{z}_a) \mathbf{\Gamma}_{0,P}^\omega(\mathbf{x} - \mathbf{z}^S) d\sigma(\mathbf{x}) \right) \overline{\mathbf{U}}(\mathbf{z}_a) \right] \right. \\ &\quad \left. + c_S \mathcal{H}^S[\mathbf{U}](\mathbf{z}^S) \cdot \left[\left(\int_{\partial\Omega} \overline{\mathbf{\Gamma}_0^\omega}(\mathbf{x} - \mathbf{z}_a) \mathbf{\Gamma}_{0,S}^\omega(\mathbf{x} - \mathbf{z}^S) d\sigma(\mathbf{x}) \right) \overline{\mathbf{U}}(\mathbf{z}_a) \right] \right). \end{aligned} \quad (4.4)$$

By using Lemma 3.2, we can easily get

$$\begin{aligned} \mathcal{I}_W[\mathbf{U}](\mathbf{z}^S) &\simeq -C\omega^3 \Re e \left(\mathcal{H}^P[\mathbf{U}](\mathbf{z}^S) \cdot \left[\Im m \{ \mathbf{\Gamma}_{0,P}^\omega(\mathbf{z}^S - \mathbf{z}_a) \} \overline{\mathbf{U}}(\mathbf{z}_a) \right] \right. \\ &\quad \left. + \mathcal{H}^S[\mathbf{U}](\mathbf{z}^S) \cdot \left[\Im m \{ \mathbf{\Gamma}_{0,S}^\omega(\mathbf{z}^S - \mathbf{z}_a) \} \overline{\mathbf{U}}(\mathbf{z}_a) \right] \right). \end{aligned} \quad (4.5)$$

Consider n uniformly distributed directions $(\mathbf{e}_{\theta_1}, \mathbf{e}_{\theta_2}, \dots, \mathbf{e}_{\theta_n})$ on the unit disk or sphere for n sufficiently large. Then, the following proposition holds.

Proposition 4.1. *Let \mathbf{U}_j^α be defined in (3.14), where $j = 1, 2, \dots, n$, for n sufficiently large. Then, for all $\mathbf{z}^S \in \Omega$ far from $\partial\Omega$,*

$$\frac{1}{n} \sum_{j=1}^n \mathcal{I}_W[\mathbf{U}_j^P](\mathbf{z}^S) \simeq 4\mu_0 C\omega^3 \left(\frac{\pi}{\kappa_P} \right)^{d-2} \left(\frac{\kappa_S}{\kappa_P} \right)^2 \left| \Im m \{ \mathbf{\Gamma}_{0,P}^\omega(\mathbf{z}^S - \mathbf{z}_a) \} \right|^2, \quad (4.6)$$

and

$$\frac{1}{n} \sum_{j=1}^n \mathcal{I}_W[\mathbf{U}_j^S](\mathbf{z}^S) \simeq 4\mu_0 C\omega^3 \left(\frac{\pi}{\kappa_S} \right)^{d-2} \left| \Im m \{ \mathbf{\Gamma}_{0,S}^\omega(\mathbf{z}^S - \mathbf{z}_a) \} \right|^2, \quad (4.7)$$

where C is given by (3.12).

Proof. By using similar arguments as in Proposition 3.3 and (4.5), we show that the weighted imaging functional \mathcal{I}_W for n plane P -waves is given by

$$\begin{aligned} \frac{1}{n} \sum_{j=1}^n \mathcal{I}_W[\mathbf{U}_j^P](\mathbf{z}^S) &= -C\omega^3 \frac{1}{n} \Re e \sum_{j=1}^n \mathbf{U}_j^P(\mathbf{z}^S) \cdot \left[\Im m \{ \mathbf{\Gamma}_{0,P}^\omega(\mathbf{z}^S - \mathbf{z}_a) \} \overline{\mathbf{U}_j^P}(\mathbf{z}_a) \right] \\ &\simeq -C\omega^3 \frac{1}{n} \Re e \sum_{j=1}^n e^{i\kappa_P(\mathbf{z}^S - \mathbf{z}_a) \cdot \mathbf{e}_{\theta_j}} \mathbf{e}_{\theta_j} \cdot \left[\Im m \{ \mathbf{\Gamma}_{0,P}^\omega(\mathbf{z}^S - \mathbf{z}_a) \} \mathbf{e}_{\theta_j} \right] \\ &\simeq 4\mu_0 C\omega^3 \left(\frac{\pi}{\kappa_P} \right)^{d-2} \left(\frac{\kappa_S}{\kappa_P} \right)^2 \left| \Im m \{ \mathbf{\Gamma}_{0,P}^\omega(\mathbf{z}^S - \mathbf{z}_a) \} \right|^2. \end{aligned}$$

For n plane S -waves

$$\begin{aligned}
\frac{1}{n} \sum_{j=1}^n \mathcal{I}_W[\mathbf{U}_j^S](\mathbf{z}^S) &= -C\omega^3 \frac{1}{n} \sum_{j=1}^n \mathbf{U}_j^S(\mathbf{z}^S) \cdot [\Im m \{ \mathbf{\Gamma}_{0,S}^\omega(\mathbf{z}^S - \mathbf{z}_a) \} \mathbf{U}_j^S(\mathbf{z}_a)] \\
&\simeq -C\omega^3 \frac{1}{n} \sum_{j=1}^n e^{i\kappa_S(\mathbf{z}^S - \mathbf{z}_a) \cdot \mathbf{e}_{\theta_j}} \mathbf{e}_{\theta_j}^\perp \cdot [\Im m \{ \mathbf{\Gamma}_{0,S}^\omega(\mathbf{z}^S - \mathbf{z}_a) \} \mathbf{e}_{\theta_j}^\perp] \\
&\simeq 4\mu_0 C\omega^3 \left(\frac{\pi}{\kappa_S}\right)^{d-2} |\Im m \{ \mathbf{\Gamma}_{0,S}^\omega(\mathbf{z}^S - \mathbf{z}_a) \}|^2,
\end{aligned}$$

where one should use the version (3.20) in dimension 3. \square

Proposition 4.1 shows that \mathcal{I}_W , attains its maximum at \mathbf{z}_a (see Figure 1) and the coupling term $\Im m \{ \mathbf{\Gamma}_{0,P}^\omega(\mathbf{z}^S - \mathbf{z}_a) \} : \Im m \{ \mathbf{\Gamma}_{0,S}^\omega(\mathbf{z}^S - \mathbf{z}_a) \}$, responsible for the decreased resolution in \mathcal{I}_{TD} , is absent. Moreover, the resolution using weighted imaging functional \mathcal{I}_W is the Rayleigh one, that is, restricted by the diffraction limit of half a wavelength of the wave impinging upon Ω , thanks to the term $|\Im m \{ \mathbf{\Gamma}_{0,\alpha}^\omega(\mathbf{z}^S - \mathbf{z}_a) \}|^2$. Finally, it is worth mentioning that \mathcal{I}_W is a topological derivative based imaging functional. In fact, it is the topological derivative of the discrepancy functional $c_S \mathcal{E}_f[\mathbf{U}^S] + c_P \mathcal{E}_f[\mathbf{U}^P]$, where \mathbf{U}^S is an S -plane wave and \mathbf{U}^P is a P -plane wave.

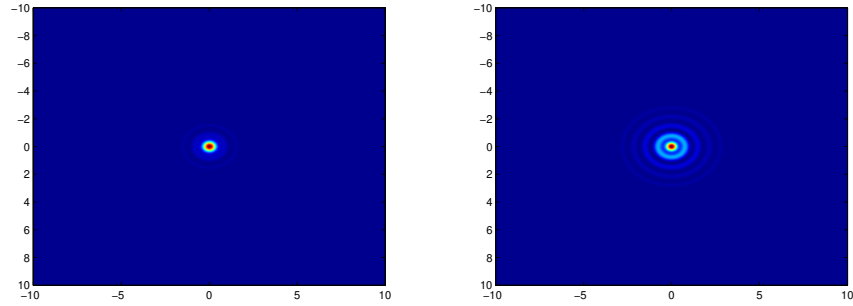


Figure 1: Typical plots of $|\Im m \{ \mathbf{\Gamma}_{0,S}^\omega(\mathbf{z}^S - \mathbf{z}_a) \}|^2$ (on the left) and $|\Im m \{ \mathbf{\Gamma}_{0,P}^\omega(\mathbf{z}^S - \mathbf{z}_a) \}|^2$ (on the right) for $\mathbf{z}_a = \mathbf{0}$ and $c_P/c_S = \sqrt{11}$.

4.2.2 Case II: Elasticity contrast

Suppose $\rho_0 = \rho_1$ and assume for simplicity that $\mathbb{M} = \mathbb{M}'(B') = \mathbb{M}(B)$. Then, the weighted imaging functional \mathcal{I}_W reduces to

$$\begin{aligned}
\mathcal{I}_W(\mathbf{z}^S) &= -\delta^d \left[c_P \nabla \mathcal{H}^P[\mathbf{U}(\mathbf{z}^S)] : \mathbb{M} \nabla \mathcal{H}^P[\mathbf{w}(\mathbf{z}^S)] + c_S \nabla \mathcal{H}^S[\mathbf{U}(\mathbf{z}^S)] : \mathbb{M} \nabla \mathcal{H}^S \mathbf{w}(\mathbf{z}^S) \right] \\
&= -\delta^d \left[c_P \nabla \mathcal{H}^P[\mathbf{U}(\mathbf{z}^S)] : \mathbb{M} \left(\int_{\partial\Omega} \nabla_{\mathbf{z}_a} \overline{\Gamma_0^\omega}(\mathbf{x} - \mathbf{z}_a) \nabla_{\mathbf{z}^S} \Gamma_{0,P}^\omega(\mathbf{x} - \mathbf{z}^S) d\sigma(\mathbf{x}) : \mathbb{M} \overline{\nabla \mathbf{U}}(\mathbf{z}_a) \right) \right. \\
&\quad \left. + c_S \nabla \mathcal{H}^S[\mathbf{U}(\mathbf{z}^S)] : \mathbb{M} \left(\int_{\partial\Omega} \nabla_{\mathbf{z}_a} \overline{\Gamma_0^\omega}(\mathbf{x} - \mathbf{z}_a) \nabla_{\mathbf{z}^S} \Gamma_{0,S}^\omega(\mathbf{x} - \mathbf{z}^S) d\sigma(\mathbf{x}) : \mathbb{M} \overline{\nabla \mathbf{U}}(\mathbf{z}_a) \right) \right] \\
&= -\delta^d \left[\nabla \mathcal{H}^P[\mathbf{U}(\mathbf{z}^S)] : \mathbb{M} \left(\Im m \{ (\nabla^2 \Gamma_{0,P}^\omega)(\mathbf{z}^S - \mathbf{z}_a) \} : \mathbb{M} \overline{\nabla \mathbf{U}}(\mathbf{z}_a) \right) \right. \\
&\quad \left. + \nabla \mathcal{H}^S[\mathbf{U}(\mathbf{z}^S)] : \mathbb{M} \left(\Im m \{ (\nabla^2 \Gamma_{0,S}^\omega)(\mathbf{z}^S - \mathbf{z}_a) \} : \mathbb{M} \overline{\nabla \mathbf{U}}(\mathbf{z}_a) \right) \right]. \tag{4.8}
\end{aligned}$$

We observed in Section 3.2.2 that the resolution of \mathcal{I}_{TD} is compromised because of the coupling term $J_{S,P}(\mathbf{z}^S)$. We can cancel out this term by using the weighted imaging functional \mathcal{I}_W . For example, using analogous arguments as in Proposition 3.4, we can easily prove the following result.

Proposition 4.2. *Let \mathbf{U}_j^α be defined in (3.14), where $j = 1, 2, \dots, n$, for n sufficiently large. Let $J_{\alpha,\beta}$ be defined by (3.24). Then, for all $\mathbf{z}^S \in \Omega$ far from $\partial\Omega$,*

$$\frac{1}{n} \sum_{j=1}^n \mathcal{I}_W[\mathbf{U}_j^\alpha](\mathbf{z}^S) \simeq 4\delta^d \frac{\mu_0}{\omega} \left(\frac{\pi}{\kappa_\alpha} \right)^{d-2} \left(\frac{\kappa_S}{\kappa_\alpha} \right)^2 J_{\alpha,\alpha}(\mathbf{z}^S), \quad \alpha \in \{P, S\}. \tag{4.9}$$

It can be established that \mathcal{I}_W attains its maximum at $\mathbf{z}^S = \mathbf{z}_a$. Consider, for example, the canonical case of a circular or spherical inclusion. The following propositions hold.

Proposition 4.3. *Let D be a disk or a sphere. Then for all search points $\mathbf{z}^S \in \Omega$,*

$$\begin{aligned}
J_{P,P}(\mathbf{z}^S) &= a^2 \left| \nabla^2 (\Im m \Gamma_{0,P}^\omega)(\mathbf{z}^S - \mathbf{z}_a) \right|^2 + 2ab \left| \Delta (\Im m \Gamma_{0,P}^\omega)(\mathbf{z}^S - \mathbf{z}_a) \right|^2 \\
&\quad + b^2 \left| \Delta \text{Tr} (\Im m \Gamma_{0,P}^\omega)(\mathbf{z}^S - \mathbf{z}_a) \right|^2, \tag{4.10}
\end{aligned}$$

where Tr represents the trace operator and the constants a and b are defined in (2.19).

Proof. Since

$$(\nabla^2 \Gamma_{0,P}^\omega)_{ijkl} = \partial_{ik} (\Gamma_{0,P}^\omega)_{jl}, \tag{4.11}$$

it follows from (2.19) that

$$\begin{aligned}
(\mathbb{M}\nabla^2\mathbf{\Gamma}_{0,P}^\omega)_{ijkl} &= \sum_{p,q} m_{ijpq} (\nabla^2\mathbf{\Gamma}_{0,P}^\omega)_{pqkl} \\
&= \frac{a}{2} \left(\partial_{ik} (\mathbf{\Gamma}_{0,P}^\omega)_{jl} + \partial_{jk} (\mathbf{\Gamma}_{0,P}^\omega)_{il} \right) + b \sum_{q=1}^d \partial_{qk} (\mathbf{\Gamma}_{0,P}^\omega)_{ql} \delta_{ij} \\
&= \frac{a}{2} \partial_k \left((\nabla\mathbf{\Gamma}_{0,P}^\omega \mathbf{e}_l)_{ij} + (\nabla\mathbf{\Gamma}_{0,P}^\omega \mathbf{e}_l)_{ij}^T \right) + b \partial_k \nabla \cdot \left((\mathbf{\Gamma}_{0,P}^\omega \mathbf{e}_l) \right) \delta_{ij}
\end{aligned} \tag{4.12}$$

where \mathbf{e}_l is the unit vector in the direction x_l .

Now, since $\mathbf{\Gamma}_{0,P}^\omega \mathbf{e}_l$ is a P -wave, its rotational part vanishes and the gradient is symmetric, *i.e.*,

$$\nabla \times (\mathbf{\Gamma}_{0,P}^\omega \mathbf{e}_l) = 0 \quad \text{and} \quad (\nabla\mathbf{\Gamma}_{0,P}^\omega \mathbf{e}_l)_{ij} = (\nabla\mathbf{\Gamma}_{0,P}^\omega \mathbf{e}_l)_{ji} = (\nabla\mathbf{\Gamma}_{0,P}^\omega \mathbf{e}_l)_{ij}^T. \tag{4.14}$$

Consequently,

$$\nabla \nabla \cdot \left((\mathbf{\Gamma}_{0,P}^\omega \mathbf{e}_l) \right) = \nabla \times \left(\nabla \times (\mathbf{\Gamma}_{0,P}^\omega \mathbf{e}_l) \right) + \Delta \left(\mathbf{\Gamma}_{0,P}^\omega \mathbf{e}_l \right) = \Delta \left(\mathbf{\Gamma}_{0,P}^\omega \mathbf{e}_l \right), \tag{4.15}$$

which, together with (4.13) and (4.14), implies

$$\mathbb{M}\nabla^2\mathbf{\Gamma}_{0,P}^\omega = a \nabla^2\mathbf{\Gamma}_{0,P}^\omega + b \mathbf{I}_2 \otimes \Delta\mathbf{\Gamma}_{0,P}^\omega. \tag{4.16}$$

Moreover, by the definition of $\mathbf{\Gamma}_{0,P}^\omega$, its Hessian, $\nabla^2\mathbf{\Gamma}_{0,P}^\omega$, is also symmetric. Indeed,

$$\left(\nabla^2\mathbf{\Gamma}_{0,P}^\omega \right)_{ijkl}^T = \partial_{ki} (\mathbf{\Gamma}_{0,P}^\omega)_{lj} = -\frac{\mu_0}{\kappa_S^2} \partial_{kijl} G_P^\omega = \left(\nabla^2\mathbf{\Gamma}_{0,P}^\omega \right)_{ijkl}. \tag{4.17}$$

Therefore, by virtue of (4.16) and (4.17), $J_{P,P}$ can be rewritten as

$$\begin{aligned}
J_{P,P}(\mathbf{z}^S) &= \left(a \Im\{(\nabla^2\mathbf{\Gamma}_{0,P}^\omega)(\mathbf{z}^S - \mathbf{z}_a)\} + b \mathbf{I}_2 \otimes \Im\{(\Delta\mathbf{\Gamma}_{0,P}^\omega)(\mathbf{z}^S - \mathbf{z}_a)\} \right) \\
&\quad : \left(a \Im\{(\nabla^2\mathbf{\Gamma}_{0,P}^\omega)(\mathbf{z}^S - \mathbf{z}_a)\} + b \Im\{(\Delta\mathbf{\Gamma}_{0,P}^\omega)(\mathbf{z}^S - \mathbf{z}_a)\} \otimes \mathbf{I}_2 \right).
\end{aligned} \tag{4.18}$$

Finally, we observe that

$$\left(\nabla^2 \Im\{ \mathbf{\Gamma}_{0,P}^\omega \} \right) : \left(\nabla^2 \Im\{ \mathbf{\Gamma}_{0,P}^\omega \} \right)^T = \left| \nabla^2 \Im\{ \mathbf{\Gamma}_{0,P}^\omega \} \right|^2, \tag{4.19}$$

$$\begin{aligned}
\nabla^2 \Im\{\mathbf{\Gamma}_{0,P}^\omega\} : (\mathbf{I}_2 \otimes \Delta \Im\{\mathbf{\Gamma}_{0,P}^\omega\}) &= \nabla^2 \Im\{\mathbf{\Gamma}_{0,P}^\omega\} : (\Delta \Im\{\mathbf{\Gamma}_{0,P}^\omega\} \otimes \mathbf{I}_2) \\
&= \sum_{i,j,k,l=1}^d \left(\Im(\partial_{ik} \mathbf{\Gamma}_{0,P}^\omega)_{jl} \right) \delta_{ij} \Delta \Im(\mathbf{\Gamma}_{0,P}^\omega)_{kl} \\
&= \sum_{k,l=1}^d \left(\sum_{i=1}^d \left(\Im(\partial_{ik} \mathbf{\Gamma}_{0,P}^\omega)_{il} \right) \right) \Delta \Im(\mathbf{\Gamma}_{0,P}^\omega)_{kl} \\
&= \sum_{k,l=1}^d \left(\Delta \Im(\mathbf{\Gamma}_{0,P}^\omega)_{kl} \right)^2 \\
&= \left| \Delta \Im\{\mathbf{\Gamma}_{0,P}^\omega\} \right|^2, \tag{4.20}
\end{aligned}$$

and

$$\begin{aligned}
(\mathbf{I}_2 \otimes \Delta \Im\{\mathbf{\Gamma}_{0,P}^\omega\}) : (\Delta \Im\{\mathbf{\Gamma}_{0,P}^\omega\} \otimes \mathbf{I}_2) &= \sum_{i,j,k,l=1}^d \delta_{ij} \Delta \Im(\mathbf{\Gamma}_{0,P}^\omega)_{kl} \delta_{kl} \Delta \Im(\mathbf{\Gamma}_{0,P}^\omega)_{ij} \\
&= \sum_{i,k=1}^d \Delta \Im(\mathbf{\Gamma}_{0,P}^\omega)_{kk} \Delta \Im(\mathbf{\Gamma}_{0,P}^\omega)_{ii} \\
&= \left| \Delta \text{Tr}(\Im\{\mathbf{\Gamma}_{0,P}^\omega\}) \right|^2. \tag{4.21}
\end{aligned}$$

We arrive at the conclusion by substituting (4.19), (4.20) and (4.21) in (4.18). \square

Proposition 4.4. *Let D be a disk or a sphere. Then, for all search points $\mathbf{z}^S \in \Omega$,*

$$\begin{aligned}
J_{S,S}(\mathbf{z}^S) &= \frac{a^2}{\mu_0^2} \left[\frac{1}{\kappa_S^4} \left| \nabla^4 \Im\{G_S^\omega(\mathbf{z}^S - \mathbf{z}_a)\} \right|^2 + \frac{(d-6)}{4} \left| \nabla^2 \Im\{G_S^\omega(\mathbf{z}^S - \mathbf{z}_a)\} \right|^2 \right. \\
&\quad \left. + \frac{\kappa_S^4}{4} \left| \Im\{G_S^\omega(\mathbf{z}^S - \mathbf{z}_a)\} \right|^2 \right] \\
&= \frac{a^2}{\mu_0^2} \left[\frac{1}{\kappa_S^4} \sum_{ijkl, k \neq l} \left| \partial_{ijkl} \Im\{G_S^\omega(\mathbf{z}^S - \mathbf{z}_a)\} \right|^2 + \frac{(d-2)}{4} \left| \nabla^2 \Im\{G_S^\omega(\mathbf{z}^S - \mathbf{z}_a)\} \right|^2 \right. \\
&\quad \left. + \frac{\kappa_S^4}{4} \left| \Im\{G_S^\omega(\mathbf{z}^S - \mathbf{z}_a)\} \right|^2 \right], \tag{4.22}
\end{aligned}$$

where a is the constant as in (2.19).

Proof. As before, we have

$$\begin{aligned}
\left(\mathbb{M} \nabla^2 \mathbf{\Gamma}_{0,S}^\omega \right)_{ijkl} &= \frac{a}{2} \left(\partial_{ik} (\mathbf{\Gamma}_{0,S}^\omega)_{jl} + \partial_{jk} (\mathbf{\Gamma}_{0,S}^\omega)_{il} \right) + b \partial_k \nabla \cdot \left((\mathbf{\Gamma}_{0,S}^\omega e_l) \right) \delta_{ij} \\
&= \frac{a}{2} \left(\partial_{ik} (\mathbf{\Gamma}_{0,S}^\omega)_{jl} + \partial_{jk} (\mathbf{\Gamma}_{0,S}^\omega)_{il} \right), \tag{4.23}
\end{aligned}$$

and

$$\left(\mathbb{M}\nabla^2\mathbf{\Gamma}_{0,S}^\omega\right)_{ijkl}^T = \frac{a}{2} \left(\partial_{ik}(\mathbf{\Gamma}_{0,S}^\omega)_{jl} + \partial_{il}(\mathbf{\Gamma}_{0,S}^\omega)_{jk}\right). \quad (4.24)$$

Here we have used the facts that $\mathbf{\Gamma}_{0,S}^\omega \mathbf{e}_l$ is a S -wave and, $\mathbf{\Gamma}_{0,S}^\omega$ and its Hessian are symmetric, *i.e.*,

$$\partial_{ik}(\mathbf{\Gamma}_{0,S}^\omega)_{jl} = \partial_{ki}(\mathbf{\Gamma}_{0,S}^\omega)_{jl} = \partial_{ik}(\mathbf{\Gamma}_{0,S}^\omega)_{lj} = \partial_{ki}(\mathbf{\Gamma}_{0,S}^\omega)_{lj}. \quad (4.25)$$

Substituting, (4.23) and (4.24) in (3.24), we obtain

$$\begin{aligned} J_{S,S}(\mathbf{z}^S) &= \frac{a^2}{4} \sum_{i,j,k,l=1}^d \Im m \left\{ ((\partial_{ik}\mathbf{\Gamma}_{0,S}^\omega)(\mathbf{z}^S - \mathbf{z}_a))_{jl} + ((\partial_{jk}\mathbf{\Gamma}_{0,S}^\omega)(\mathbf{z}^S - \mathbf{z}_a))_{il} \right\} \\ &\quad \times \Im m \left\{ ((\partial_{ik}\mathbf{\Gamma}_{0,S}^\omega)(\mathbf{z}^S - \mathbf{z}_a))_{jl} + ((\partial_{il}\mathbf{\Gamma}_{0,S}^\omega)(\mathbf{z}^S - \mathbf{z}_a))_{jk} \right\} \\ &:= \frac{a^2}{4} (T_1(\mathbf{z}^S) + 2T_2(\mathbf{z}^S) + T_3(\mathbf{z}^S)), \end{aligned} \quad (4.26)$$

where

$$\begin{cases} T_1(\mathbf{z}^S) &= \sum_{i,j,k,l=1}^d \left(\Im m \left\{ (\partial_{ik}\mathbf{\Gamma}_{0,S}^\omega)_{jl}(\mathbf{z}^S - \mathbf{z}_a) \right\} \right) \left(\Im m \left\{ (\partial_{ik}\mathbf{\Gamma}_{0,S}^\omega)_{jl}(\mathbf{z}^S - \mathbf{z}_a) \right\} \right), \\ T_2(\mathbf{z}^S) &= \sum_{i,j,k,l=1}^d \left(\Im m \left\{ (\partial_{ik}\mathbf{\Gamma}_{0,S}^\omega)_{jl}(\mathbf{z}^S - \mathbf{z}_a) \right\} \right) \left(\Im m \left\{ (\partial_{il}\mathbf{\Gamma}_{0,S}^\omega)_{jk}(\mathbf{z}^S - \mathbf{z}_a) \right\} \right), \\ T_3(\mathbf{z}^S) &= \sum_{i,j,k,l=1}^d \left(\Im m \left\{ (\partial_{jk}\mathbf{\Gamma}_{0,S}^\omega)_{il}(\mathbf{z}^S - \mathbf{z}_a) \right\} \right) \left(\Im m \left\{ (\partial_{il}\mathbf{\Gamma}_{0,S}^\omega)_{jk}(\mathbf{z}^S - \mathbf{z}_a) \right\} \right). \end{cases}$$

Notice that

$$\Im m \left\{ \mathbf{\Gamma}_{0,S}^\omega(\mathbf{x}) \right\} = \frac{1}{\mu_0 \kappa_S^2} (\kappa_S^2 \mathbf{I}_2 + \mathbb{D}_{\mathbf{x}}) \Im m \left\{ G_S^\omega(\mathbf{x}) \right\},$$

and $\Im m \{G_S^\omega\}$ satisfies

$$\Delta \Im m \{G_S^\omega\}(\mathbf{z}^S - \mathbf{z}_a) + \kappa_S^2 \Im m \{G_S^\omega\}(\mathbf{z}^S - \mathbf{z}_a) = 0 \quad \text{for } \mathbf{z}^S \neq \mathbf{z}_a. \quad (4.27)$$

Therefore, the first term T_1 can be computed as follows

$$\begin{aligned} T_1(\mathbf{z}^S) &= \left| \nabla^2 (\Im m \mathbf{\Gamma}_{0,S}^\omega)(\mathbf{z}^S - \mathbf{z}_a) \right|^2 \\ &= \frac{1}{\mu_0^2 \kappa_S^4} \sum_{i,j,k,l=1}^d \left[\left(\partial_{ijkl} (\Im m G_S^\omega)(\mathbf{z}^S - \mathbf{z}_a) \right)^2 + \kappa_S^4 \delta_{jl} \left(\partial_{ik} (\Im m G_S^\omega)(\mathbf{z}^S - \mathbf{z}_a) \right)^2 \right. \\ &\quad \left. + 2\kappa_S^2 \delta_{jl} \partial_{ik} (\Im m G_S^\omega)(\mathbf{z}^S - \mathbf{z}_a) \partial_{ijkl} (\Im m G_S^\omega)(\mathbf{z}^S - \mathbf{z}_a) \right]. \end{aligned}$$

We also have

$$\begin{aligned}
& \sum_{i,j,k,l=1}^d 2\delta_{jl}\partial_{ik}(\Im m G_S^\omega)(\mathbf{z}^S - \mathbf{z}_a) \left(\partial_{ijkl}(\Im m G_S^\omega)(\mathbf{z}^S - \mathbf{z}_a) \right) \\
&= 2 \sum_{i,k=1}^d \left(\partial_{ik}(\Im m G_S^\omega)(\mathbf{z}^S - \mathbf{z}_a) \right) \left(\partial_{ik} \sum_{l=1}^d \partial_{il}(\Im m G_S^\omega)(\mathbf{z}^S - \mathbf{z}_a) \right) \\
&= -2\kappa_S^2 \sum_{i,k=1}^d \left(\partial_{ik}(\Im m G_S^\omega)(\mathbf{z}^S - \mathbf{z}_a) \right)^2,
\end{aligned}$$

and

$$\sum_{i,j,k,l=1}^d \delta_{jl} \left(\partial_{ik}(\Im m G_S^\omega)(\mathbf{z}^S - \mathbf{z}_a) \right)^2 = d \sum_{i,k=1}^d \left(\partial_{ik}(\Im m G_S^\omega)(\mathbf{z}^S - \mathbf{z}_a) \right)^2.$$

Consequently, we have

$$\begin{aligned}
T_1(\mathbf{z}^S) &= \left| \nabla^2(\Im m \mathbf{\Gamma}_{0,S}^\omega)(\mathbf{z}^S - \mathbf{z}_a) \right|^2 = \frac{1}{\mu_0^2 \kappa_S^4} \left| \nabla^4(\Im m G_S^\omega)(\mathbf{z}^S - \mathbf{z}_a) \right|^2 \\
&\quad + \frac{(d-2)}{\mu_0^2} \sum_{i,k=1}^d \left(\partial_{ik}(\Im m G_S^\omega)(\mathbf{z}^S - \mathbf{z}_a) \right)^2.
\end{aligned} \tag{4.28}$$

Estimation of the term T_2 is quite similar. Indeed,

$$\begin{aligned}
T_2(\mathbf{z}^S) &= \frac{1}{\mu_0^2 \kappa_S^4} \sum_{i,j,k,l=1}^d \left[\left(\partial_{ijkl}(\Im m G_S^\omega)(\mathbf{z}^S - \mathbf{z}_a) \right)^2 \right. \\
&\quad \left. + 2\kappa_S^2 \delta_{jl} \partial_{ik}(\Im m G_S^\omega)(\mathbf{z}^S - \mathbf{z}_a) \partial_{ijkl}(\Im m G_S^\omega)(\mathbf{z}^S - \mathbf{z}_a) \right. \\
&\quad \left. + \kappa_S^4 \delta_{jl} \delta_{jk} \left(\partial_{ik}(\Im m G_S^\omega)(\mathbf{z}^S - \mathbf{z}_a) \right) \left(\partial_{il}(\Im m G_S^\omega)(\mathbf{z}^S - \mathbf{z}_a) \right) \right].
\end{aligned}$$

Finally, using

$$\sum_{i,j,k,l=1}^d \delta_{jl} \delta_{jk} \left(\partial_{ik}(\Im m G_S^\omega)(\mathbf{z}^S - \mathbf{z}_a) \right) \left(\partial_{il}(\Im m G_S^\omega)(\mathbf{z}^S - \mathbf{z}_a) \right) = \sum_{i,k=1}^d \left(\partial_{ik}(\Im m G_S^\omega)(\mathbf{z}^S - \mathbf{z}_a) \right)^2,$$

we obtain that

$$T_2(\mathbf{z}^S) = \frac{1}{\mu_0^2 \kappa_S^4} \left| \nabla^4(\Im m G_S^\omega)(\mathbf{z}^S - \mathbf{z}_a) \right|^2 - \frac{1}{\mu_0^2} \left| \nabla^2(\Im m G_S^\omega)(\mathbf{z}^S - \mathbf{z}_a) \right|^2. \tag{4.29}$$

Similarly,

$$\begin{aligned}
T_3(\mathbf{z}^S) &= \frac{1}{\mu_0^2 \kappa_S^4} \sum_{i,j,k,l=1}^d \left[\left(\partial_{ijkl} (\Im m G_S^\omega)(\mathbf{z}^S - \mathbf{z}_a) \right)^2 \right. \\
&\quad + 2\kappa_S^2 \delta_{jl} \partial_{ik} (\Im m G_S^\omega)(\mathbf{z}^S - \mathbf{z}_a) \left(\partial_{ijkl} (\Im m G_S^\omega)(\mathbf{z}^S - \mathbf{z}_a) \right) \\
&\quad \left. + \kappa_S^4 \delta_{il} \delta_{jk} \left(\partial_{jk} (\Im m G_S^\omega)(\mathbf{z}^S - \mathbf{z}_a) \right) \left(\partial_{il} (\Im m G_S^\omega)(\mathbf{z}^S - \mathbf{z}_a) \right) \right].
\end{aligned}$$

By virtue of

$$\begin{aligned}
&\sum_{i,j,k,l=1}^d \delta_{il} \delta_{jk} \left(\partial_{jk} (\Im m G_S^\omega)(\mathbf{z}^S - \mathbf{z}_a) \right) \left(\partial_{il} (\Im m G_S^\omega)(\mathbf{z}^S - \mathbf{z}_a) \right) \\
&= \sum_{i,k=1}^d \left(\partial_{kk} (\Im m G_S^\omega)(\mathbf{z}^S - \mathbf{z}_a) \right) \left(\partial_{ii} (\Im m G_S^\omega)(\mathbf{z}^S - \mathbf{z}_a) \right) \\
&= \kappa_S^4 \left(\Im m G_S^\omega(\mathbf{z}^S - \mathbf{z}_a) \right)^2,
\end{aligned}$$

we have

$$\begin{aligned}
T_3(\mathbf{z}^S) &= \frac{1}{\mu_0^2 \kappa_S^4} \left| \nabla^4 (\Im m G_S^\omega)(\mathbf{z}^S - \mathbf{z}_a) \right|^2 - \frac{2}{\mu_0^2} \left| \nabla^2 (\Im m G_S^\omega)(\mathbf{z}^S - \mathbf{z}_a) \right|^2 \\
&\quad + \frac{\kappa_S^4}{\mu_0^2} \left| \Im m G_S^\omega(\mathbf{z}^S - \mathbf{z}_a) \right|^2.
\end{aligned} \tag{4.30}$$

We conclude the proof by substituting (4.28), (4.29) and (4.30) in (4.26) and using again (4.27). \square

Figure 2 shows typical plots of $J_{\alpha,\alpha}$ for $\alpha \in \{P, S\}$.

5 Statistical stability with measurement noise

Let \mathbf{U}_j^P and \mathbf{U}_j^S be as before. Let $\{\mathbf{U}_j\}$ be plane waves. Define

$$\mathcal{I}_{\text{WF}}[\{\mathbf{U}_j\}](\mathbf{z}^S) = \frac{1}{n} \sum_{j=1}^n \mathcal{I}_{\text{W}}[\mathbf{U}_j](\mathbf{z}^S). \tag{5.1}$$

In the previous section, we have analyzed the resolution of the imaging functional \mathcal{I}_{WF} in the ideal situation where the measurement \mathbf{u}_{meas} is accurate. Here, we analyze how the result will be modified when the measurement is corrupted by noise.

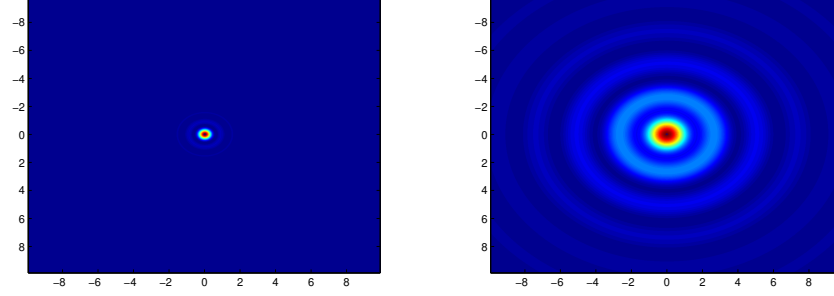


Figure 2: Typical plots of J_{SS} (on the right) and J_{PP} (on the right) for $\mathbf{z}_a = \mathbf{0}$ and $c_P/c_S = \sqrt{11}$.

5.1 Measurement noise model

We consider the simplest model for the measurement noise. Let \mathbf{u}_{true} be the accurate value of the elastic displacement field. The measurement \mathbf{u}_{meas} is then

$$\mathbf{u}_{\text{meas}}(\mathbf{x}) = \mathbf{u}_{\text{true}}(\mathbf{x}) + \boldsymbol{\nu}_{\text{noise}}(\mathbf{x}), \quad (5.2)$$

that is the accurate value corrupted by measurement noise modeled as $\boldsymbol{\nu}_{\text{noise}}(\mathbf{x})$, $\mathbf{x} \in \partial\Omega$. Note that $\boldsymbol{\nu}_{\text{noise}}(\mathbf{x})$ is valued in \mathbb{C}^d , $d = 2, 3$.

Let \mathbb{E} denote the expectation with respect to the statistics of the measurement noise. We assume that $\{\boldsymbol{\nu}_{\text{noise}}(\mathbf{x}), \mathbf{x} \in \partial\Omega\}$ is mean zero circular Gaussian and satisfies

$$\mathbb{E}[\boldsymbol{\nu}_{\text{noise}}(\mathbf{y}) \otimes \overline{\boldsymbol{\nu}_{\text{noise}}(\mathbf{y}')}^T] = \sigma_{\text{noise}}^2 \delta_{\mathbf{y}}(\mathbf{y}') \mathbf{I}_2. \quad (5.3)$$

This means that firstly the measurement noises at different locations on the boundary are uncorrelated; secondly, different components of the measurement noise are uncorrelated, and thirdly the real and imaginary parts are uncorrelated. Finally, the noise has variance σ_{noise}^2 .

In the imaging functional \mathcal{I}_{WF} , the elastic medium is probed by multiple plane waves with different propagating directions, and consequently multiple measurements are obtained at the boundary accordingly. We assume that two measurements corresponding to two different plane wave propagations are uncorrelated. Therefore, it holds that

$$\mathbb{E}[\boldsymbol{\nu}_{\text{noise}}^j(\mathbf{y}) \otimes \overline{\boldsymbol{\nu}_{\text{noise}}^l(\mathbf{y}')}] = \sigma_{\text{noise}}^2 \delta_{jl} \delta_{\mathbf{y}}(\mathbf{y}') \mathbf{I}_2, \quad (5.4)$$

where j and l are labels for the measurements and δ_{jl} is the Kronecker symbol.

5.2 Propagation of measurement noise in the back-propagation step

The measurement noise affects the topological derivative based imaging functional through the back-propagation step which builds the function \mathbf{w} in (3.6). Due to the noise, we have

$$\mathbf{w}(\mathbf{x}) = \mathcal{S}_{\Omega}^{\omega} \left[\left(\frac{1}{2} I - \mathcal{K}_{\Omega}^{\omega} \right) [\mathbf{U} - \mathbf{u}_{\text{true}} - \boldsymbol{\nu}_{\text{noise}}] \right] (\mathbf{x}) = \mathbf{w}_{\text{true}}(\mathbf{x}) + \mathbf{w}_{\text{noise}}(\mathbf{x}), \quad (5.5)$$

for $\mathbf{x} \in \Omega$. Here, \mathbf{w}_{true} is the result of back-propagating only the accurate data while $\mathbf{w}_{\text{noise}}$ is that of back-propagating the measurement noise. In particular,

$$\mathbf{w}_{\text{noise}}(\mathbf{x}) = -\mathcal{S}_{\Omega}^{\omega} \left[\overline{\left(\frac{1}{2}I - \mathcal{K}_{\Omega}^{\omega} \right) [\boldsymbol{\nu}_{\text{noise}}]} \right](\mathbf{x}), \quad \mathbf{x} \in \Omega. \quad (5.6)$$

To analyze the statistics of $\mathbf{w}_{\text{noise}}$, we proceed in two steps. First define

$$\boldsymbol{\nu}_{\text{noise},1}(\mathbf{x}) = \left(\frac{1}{2}I - \mathcal{K}_{\Omega}^{\omega} \right) [\boldsymbol{\nu}_{\text{noise}}](\mathbf{x}), \quad \mathbf{x} \in \partial\Omega. \quad (5.7)$$

Then, due to linearity, $\boldsymbol{\nu}_{\text{noise},1}$ is also a mean-zero circular Gaussian random process. Its covariance function can be calculated as

$$\begin{aligned} \mathbb{E}[\boldsymbol{\nu}_{\text{noise},1}(\mathbf{y}) \otimes \overline{\boldsymbol{\nu}_{\text{noise},1}(\mathbf{y}')}] &= \frac{1}{4} \mathbb{E}[\boldsymbol{\nu}_{\text{noise}}(\mathbf{y}) \otimes \overline{\boldsymbol{\nu}_{\text{noise}}(\mathbf{y}')}] - \frac{1}{2} \mathbb{E}[\mathcal{K}_{\Omega}^{\omega}[\boldsymbol{\nu}_{\text{noise}}](\mathbf{y}) \otimes \overline{\boldsymbol{\nu}_{\text{noise}}(\mathbf{y}')}] \\ &\quad - \frac{1}{2} \mathbb{E}[\boldsymbol{\nu}_{\text{noise}}(\mathbf{y}) \otimes \overline{\mathcal{K}_{\Omega}^{\omega}[\boldsymbol{\nu}_{\text{noise}}](\mathbf{y}')}] + \mathbb{E}[\mathcal{K}_{\Omega}^{\omega}[\boldsymbol{\nu}_{\text{noise}}](\mathbf{y}) \otimes \overline{\mathcal{K}_{\Omega}^{\omega}[\boldsymbol{\nu}_{\text{noise}}](\mathbf{y}')}]. \end{aligned}$$

The terms on the right-hand side can be evaluated using the statistics of $\boldsymbol{\nu}_{\text{noise}}$ and the explicit expression of $\mathcal{K}_{\Omega}^{\omega}$. Let us calculate the last term. It has the expression

$$\mathbb{E} \left[\int_{\partial\Omega} \int_{\partial\Omega} \left[\frac{\partial \boldsymbol{\Gamma}_0^{\omega}}{\partial \nu_{\mathbf{x}}}(\mathbf{y} - \mathbf{x}) \boldsymbol{\nu}_{\text{noise}}(\mathbf{x}) \right] \otimes \overline{\left[\frac{\partial \boldsymbol{\Gamma}_0^{\omega}}{\partial \nu_{\mathbf{x}'}}(\mathbf{y}' - \mathbf{x}') \boldsymbol{\nu}_{\text{noise}}(\mathbf{x}') \right]} d\sigma(\mathbf{x}) d\sigma(\mathbf{x}') \right].$$

Using the coordinate representations and the summation convention, we can calculate the j th element of this matrix by

$$\begin{aligned} &\int_{\partial\Omega} \int_{\partial\Omega} \left[\frac{\partial \boldsymbol{\Gamma}_0^{\omega}}{\partial \nu_{\mathbf{x}}}(\mathbf{y} - \mathbf{x}) \right]_{jl} \left[\frac{\partial \overline{\boldsymbol{\Gamma}_0^{\omega}}}{\partial \nu_{\mathbf{x}'}}(\mathbf{y}' - \mathbf{x}') \right]_{ks} \mathbb{E}[\boldsymbol{\nu}_{\text{noise}}(\mathbf{x}) \otimes \overline{\boldsymbol{\nu}_{\text{noise}}(\mathbf{x}')}]_{ls} d\sigma(\mathbf{x}) d\sigma(\mathbf{x}') \\ &= \sigma_{\text{noise}}^2 \int_{\partial\Omega} \left[\frac{\partial \boldsymbol{\Gamma}_0^{\omega}}{\partial \nu_{\mathbf{x}}}(\mathbf{y} - \mathbf{x}) \right]_{js} \left[\frac{\partial \overline{\boldsymbol{\Gamma}_0^{\omega}}}{\partial \nu_{\mathbf{x}}}(\mathbf{y}' - \mathbf{x}) \right]_{ks} d\sigma(\mathbf{x}) \\ &= \sigma_{\text{noise}}^2 \int_{\partial\Omega} \frac{\partial \boldsymbol{\Gamma}_0^{\omega}}{\partial \nu_{\mathbf{x}}}(\mathbf{y} - \mathbf{x}) \frac{\partial \overline{\boldsymbol{\Gamma}_0^{\omega}}}{\partial \nu_{\mathbf{x}}}(\mathbf{x} - \mathbf{y}') d\sigma(\mathbf{x}). \end{aligned}$$

In the last step, we used the reciprocity relation

$$\boldsymbol{\Gamma}_0^{\omega}(\mathbf{y} - \mathbf{x}) = [\boldsymbol{\Gamma}_0^{\omega}(\mathbf{x} - \mathbf{y})]^T, \quad (5.8)$$

for any $\mathbf{x}, \mathbf{y} \in \mathbb{R}^d$.

The other terms in the covariance function of $\boldsymbol{\nu}_{\text{noise},1}$ can be similarly calculated. Consequently, we have

$$\begin{aligned} \mathbb{E}[\boldsymbol{\nu}_{\text{noise},1}(\mathbf{y}) \otimes \overline{\boldsymbol{\nu}_{\text{noise},1}(\mathbf{y}')}] &= \frac{\sigma_{\text{noise}}^2}{4} \delta_{\mathbf{y}}(\mathbf{y}') \mathbf{I}_2 - \frac{\sigma_{\text{noise}}^2}{2} \left[\frac{\partial \boldsymbol{\Gamma}_0^{\omega}}{\partial \nu_{\mathbf{y}'}}(\mathbf{y} - \mathbf{y}') + \frac{\partial \overline{\boldsymbol{\Gamma}_0^{\omega}}}{\partial \nu_{\mathbf{y}}}(\mathbf{y} - \mathbf{y}') \right] \\ &\quad + \sigma_{\text{noise}}^2 \int_{\partial\Omega} \frac{\partial \boldsymbol{\Gamma}_0^{\omega}}{\partial \nu_{\mathbf{x}}}(\mathbf{y} - \mathbf{x}) \frac{\partial \overline{\boldsymbol{\Gamma}_0^{\omega}}}{\partial \nu_{\mathbf{x}}}(\mathbf{x} - \mathbf{y}') d\sigma(\mathbf{x}). \end{aligned} \quad (5.9)$$

From the expression of \mathcal{I}_{WF} and \mathcal{I}_{W} , we see that only the Helmholtz decomposition of \mathbf{w}_{meas} , that is $\mathcal{H}^P[\mathbf{w}]$ and $\mathcal{H}^S[\mathbf{w}]$, are used in the imaging functional. Define $\mathbf{w}^{\alpha} =$

$\mathcal{H}^\alpha[\mathbf{w}], \alpha \in \{P, S\}$. Using the decomposition in (5.5), we can similarly define $\mathbf{w}_{\text{true}}^\alpha$ and $\mathbf{w}_{\text{noise}}^\alpha$. In particular, we find that

$$\mathbf{w}_{\text{noise}}^\alpha(\mathbf{x}) = - \int_{\partial\Omega} \mathbf{\Gamma}_{0,\alpha}^\omega(\mathbf{x} - \mathbf{y}) \overline{\boldsymbol{\nu}_{\text{noise},1}(\mathbf{y})} d\sigma(\mathbf{y}), \quad \mathbf{x} \in \Omega.$$

This is a mean zero \mathbb{C}^d -valued circular Gaussian random field with parameters in Ω . The jk th element of its covariance function is evaluated by

$$\mathbb{E}[\mathbf{w}_{\text{noise}}^\alpha(\mathbf{x}) \otimes \overline{\mathbf{w}_{\text{noise}}^\alpha}(\mathbf{x}')]_{jk} = \sum_{l,s} \int_{(\partial\Omega)^2} (\mathbf{\Gamma}_{0,\alpha}^\omega(\mathbf{x} - \mathbf{y}))_{jl} (\overline{\mathbf{\Gamma}_{0,\alpha}^\omega}(\mathbf{x}' - \mathbf{y}'))_{ks} \mathbb{E}[\overline{\boldsymbol{\nu}_{\text{noise},1}(\mathbf{y})} \otimes \boldsymbol{\nu}_{\text{noise},1}(\mathbf{y}')]_{ls}.$$

Using the statistics of $\boldsymbol{\nu}_{\text{noise},1}$ derived above, we find that

$$\begin{aligned} \mathbb{E}[\mathbf{w}_{\text{noise}}^\alpha(\mathbf{x}) \otimes \overline{\mathbf{w}_{\text{noise}}^\alpha}(\mathbf{x}')] &= \frac{\sigma_{\text{noise}}^2}{4} \int_{\partial\Omega} \mathbf{\Gamma}_{0,\alpha}^\omega(\mathbf{x} - \mathbf{y}) \overline{\mathbf{\Gamma}_{0,\alpha}^\omega}(\mathbf{y} - \mathbf{x}') d\sigma(\mathbf{y}) \\ &- \frac{\sigma_{\text{noise}}^2}{2} \int_{(\partial\Omega)^2} \mathbf{\Gamma}_{0,\alpha}^\omega(\mathbf{x} - \mathbf{y}) \left[\frac{\partial \mathbf{\Gamma}_0^\omega}{\partial \nu_{\mathbf{y}}}(\mathbf{y} - \mathbf{y}') + \frac{\partial \overline{\mathbf{\Gamma}_0^\omega}}{\partial \nu_{\mathbf{y}'}}(\mathbf{y} - \mathbf{y}') \right] \overline{\mathbf{\Gamma}_{0,\alpha}^\omega}(\mathbf{y}' - \mathbf{x}') d\sigma(\mathbf{y}) d\sigma(\mathbf{y}') \\ &+ \sigma_{\text{noise}}^2 \int_{(\partial\Omega)^3} \mathbf{\Gamma}_{0,\alpha}^\omega(\mathbf{x} - \mathbf{y}) \frac{\partial \overline{\mathbf{\Gamma}_0^\omega}}{\partial \nu_{\mathbf{z}}}(\mathbf{y} - \mathbf{z}) \frac{\partial \mathbf{\Gamma}_0^\omega}{\partial \nu_{\mathbf{z}}}(\mathbf{z} - \mathbf{y}') \overline{\mathbf{\Gamma}_{0,\alpha}^\omega}(\mathbf{y}' - \mathbf{x}') d\sigma(\mathbf{z}) d\sigma(\mathbf{y}) d\sigma(\mathbf{y}'). \end{aligned}$$

Thanks to the Helmholtz-Kirchhoff identities, the above expression is simplified to

$$\begin{aligned} \mathbb{E}[\mathbf{w}_{\text{noise}}^\alpha(\mathbf{x}) \otimes \overline{\mathbf{w}_{\text{noise}}^\alpha}(\mathbf{x}')] &= - \frac{\sigma_{\text{noise}}^2}{4c_\alpha\omega} \Im m\{\mathbf{\Gamma}_{0,\alpha}^\omega(\mathbf{x} - \mathbf{x}')\} \\ &+ \frac{\sigma_{\text{noise}}^2}{2c_\alpha\omega} \int_{\partial\Omega} \mathbf{\Gamma}_{0,\alpha}^\omega(\mathbf{x} - \mathbf{y}) \frac{\partial \Im m\{\mathbf{\Gamma}_{0,\alpha}^\omega(\mathbf{y} - \mathbf{x}')\}}{\partial \nu_{\mathbf{y}}} d\sigma(\mathbf{y}) \\ &+ \frac{\sigma_{\text{noise}}^2}{2c_\alpha\omega} \int_{\partial\Omega} \frac{\partial \Im m\{\mathbf{\Gamma}_{0,\alpha}^\omega(\mathbf{x} - \mathbf{y}')\}}{\partial \nu_{\mathbf{y}'}} \overline{\mathbf{\Gamma}_{0,\alpha}^\omega}(\mathbf{y}' - \mathbf{x}') d\sigma(\mathbf{y}') \\ &- \frac{\sigma_{\text{noise}}^2}{(c_\alpha\omega)^2} \int_{\partial\Omega} \frac{\partial \Im m\{\mathbf{\Gamma}_{0,\alpha}^\omega(\mathbf{x} - \mathbf{z})\}}{\partial \nu_{\mathbf{z}}} \frac{\partial \Im m\{\mathbf{\Gamma}_{0,\alpha}^\omega(\mathbf{z} - \mathbf{x}')\}}{\partial \nu_{\mathbf{z}}} d\sigma(\mathbf{z}). \end{aligned}$$

Assuming that \mathbf{x}, \mathbf{x}' are far away from the boundary, we have from [3] the asymptotic formula that

$$\frac{\partial \mathbf{\Gamma}_{0,\alpha}^\omega(\mathbf{x} - \mathbf{y})}{\partial \nu_{\mathbf{y}}} \simeq ic_\alpha\omega \mathbf{\Gamma}_{0,\alpha}^\omega(\mathbf{x} - \mathbf{y}), \quad (5.10)$$

where the error is of order $o(|\mathbf{x} - \mathbf{y}|^{1/2-d})$. Using this asymptotic formula and the Helmholtz-Kirchhoff identity (taking the imaginary part of the identity), we obtain that

$$\mathbb{E}[\mathbf{w}_{\text{noise}}^\alpha(\mathbf{x}) \otimes \overline{\mathbf{w}_{\text{noise}}^\alpha}(\mathbf{x}')] = - \frac{\sigma_{\text{noise}}^2}{4c_\alpha\omega} \Im m\{\mathbf{\Gamma}_{0,\alpha}^\omega(\mathbf{x} - \mathbf{x}')\}. \quad (5.11)$$

In conclusion, the random field $\mathbf{w}_{\text{noise}}^\alpha(\mathbf{x}), \mathbf{x} \in \Omega$, is a Gaussian field with mean zero and covariance function (5.11). It is a speckle pattern, *i.e.*, a random cloud of hot spots where typical diameters are of the order of the wavelength and whose typical amplitudes are of the order of $\sigma_{\text{noise}}/(2\sqrt{c_\alpha\omega})$.

5.3 Stability analysis

Now we are ready to analyze the statistical stability of the imaging functional \mathcal{I}_{WF} . As before, we consider separate cases where the medium has only density contrast or only elastic contrast.

5.3.1 Case I: Density contrast

Using the facts that the plane waves \mathbf{U}^P 's are irrotational and that the plane waves \mathbf{U}^S 's are solenoidal, we see that for a searching point $\mathbf{z} \in \Omega$, and $\alpha \in \{P, S\}$,

$$\mathcal{I}_{\text{WF}}[\{\mathbf{U}_j^\alpha\}](\mathbf{z}) = c_\alpha \omega^2 \left(\frac{\rho'_1}{\rho_0} - 1 \right) |B'| \frac{1}{n} \sum_{j=1}^n \Re \{ \mathbf{U}_j^\alpha(\mathbf{z}) \cdot (\mathbf{w}_{j,\text{true}}^\alpha(\mathbf{z}) + \mathbf{w}_{j,\text{noise}}^\alpha(\mathbf{z})) \}.$$

We observe the following: The contribution of $\{\mathbf{w}_{j,\text{true}}^\alpha\}$ are exactly those in Proposition 4.1. On the other hand, the contribution of $\{\mathbf{w}_{j,\text{noise}}^\alpha\}$ forms a field corrupting the true image. With $C_\alpha := c_\alpha \omega^2 |B'| (\rho'_1 / \rho_0 - 1)$, the covariance function of the corrupted image, can be calculated as follows. Let $\mathbf{z}' \in \Omega$. We have

$$\begin{aligned} \text{Cov}(\mathcal{I}_{\text{WF}}[\{\mathbf{U}_j^\alpha\}](\mathbf{z}), \mathcal{I}_{\text{WF}}[\{\mathbf{U}_j^\alpha\}](\mathbf{z}')) &= C_\alpha^2 \frac{1}{n^2} \sum_{j,l=1}^n \mathbb{E}[\Re \{ \mathbf{U}_j^\alpha \cdot \mathbf{w}_{j,\text{noise}}^\alpha \} \Re \{ \mathbf{U}_l^\alpha \cdot \mathbf{w}_{l,\text{noise}}^\alpha \}] \\ &= C_\alpha^2 \frac{1}{2n^2} \sum_{j=1}^n \Re \left\{ \mathbf{U}_j^\alpha(\mathbf{z}) \cdot \mathbb{E}[\mathbf{w}_{j,\text{noise}}^\alpha(\mathbf{z}) \otimes \overline{\mathbf{w}_{j,\text{noise}}^\alpha(\mathbf{z}')} \overline{\mathbf{U}_j^\alpha(\mathbf{z}')}] \right\}. \end{aligned}$$

To get the second equality, we used the fact that $\mathbf{w}_{j,\text{noise}}^\alpha$ and $\mathbf{w}_{l,\text{noise}}^\alpha$ are uncorrelated unless $j = l$. Thanks to the statistics (5.11), the covariance of the image is given by

$$-C_\alpha^2 \frac{\sigma_{\text{noise}}^2}{4c_\alpha \omega} \frac{1}{2n^2} \Re \sum_{j=1}^n e^{i\kappa_\alpha(\mathbf{z}-\mathbf{z}') \cdot \mathbf{e}_{\theta_j}} \mathbf{e}_{\theta_j}^\alpha \cdot [\Im \{ \mathbf{\Gamma}_{0,\alpha}^\omega(\mathbf{z} - \mathbf{z}') \} \mathbf{e}_{\theta_j}^\alpha],$$

where $\mathbf{e}_{\theta_j}^P = \mathbf{e}_{\theta_j}$ and $\mathbf{e}_{\theta_j}^S = \mathbf{e}_{\theta_j}^\perp$.

Using the same arguments as those in the proof of Proposition 4.1, we obtain that

$$\text{Cov}(\mathcal{I}_{\text{WF}}[\{\mathbf{U}_j^\alpha\}](\mathbf{z}), \mathcal{I}_{\text{WF}}[\{\mathbf{U}_j^\alpha\}](\mathbf{z}')) = C_\alpha' \frac{\sigma_{\text{noise}}^2}{2n} |\Im \{ \mathbf{\Gamma}_{0,\alpha}^\omega(\mathbf{z} - \mathbf{z}') \}|^2, \quad (5.12)$$

where the constant

$$C_\alpha' = c_\alpha \omega^3 \mu_0 |B'|^2 \left(\frac{\rho'_1}{\rho_0} - 1 \right)^2 \left(\frac{\pi}{\kappa_\alpha} \right)^{d-2} \left(\frac{\kappa_S}{\kappa_\alpha} \right)^2.$$

The following remarks hold. Firstly, the perturbation due to noise has small typical values of order $\sigma_{\text{noise}}/\sqrt{2n}$ and slightly affects the peak of the imaging functional \mathcal{I}_{WF} . Secondly, the typical shape of the hot spot in the perturbation due to the noise is exactly of the form of the main peak of \mathcal{I}_{WF} obtained in the absence of noise. Thirdly, the use of multiple directional plane waves reduces the effect of measurement noise on the image quality.

From (5.12) it follows that the variance of the imaging functional \mathcal{I}_{WF} at the search point \mathbf{z} is given by

$$\text{Var}(\mathcal{I}_{\text{WF}}[\{\mathbf{U}_j^\alpha\}](\mathbf{z})) = C_\alpha' \frac{\sigma_{\text{noise}}^2}{2n} |\Im \{ \mathbf{\Gamma}_{0,\alpha}^\omega(\mathbf{0}) \}|^2. \quad (5.13)$$

Define the Signal-to-Noise Ratio (SNR) by

$$\text{SNR} := \frac{\mathbb{E}[\mathcal{I}_{\text{WF}}[\{\mathbf{U}_j^\alpha\}](\mathbf{z}_a)]}{\text{Var}(\mathcal{I}_{\text{WF}}[\{\mathbf{U}_j^\alpha\}](\mathbf{z}_a))^{1/2}},$$

where \mathbf{z}_a is the true location of the inclusion. From (4.6), (4.7), and (5.13), we have

$$\text{SNR} = \frac{4\sqrt{2\pi^{d-2}n\omega^{5-d}\rho_0^3c_\alpha^{d-1}\delta^d|B||\rho_1 - \rho_0|}}{\sigma_{\text{noise}}} |\Im\{\mathbf{\Gamma}_{0,\alpha}^\omega(\mathbf{0})\}|. \quad (5.14)$$

From (5.14), the SNR is proportional to the contrast $|\rho_1 - \rho_0|$ and the volume of the inclusion $\delta^d|B|$, over the standard deviation of the noise, σ_{noise} .

5.3.2 Case II: Elasticity contrast

In the case of elastic contrast, the imaging functional becomes for $\mathbf{z} \in \Omega$

$$\mathcal{I}_{\text{WF}}[\{\mathbf{U}_j^\alpha\}](\mathbf{z}) = c_\alpha \frac{1}{n} \sum_{j=1}^n \nabla \mathbf{U}_j^\alpha(\mathbf{z}) : \mathbb{M}'(B')(\nabla \mathbf{w}_{j,\text{true}}^\alpha(\mathbf{z}) + \nabla \mathbf{w}_{j,\text{noise}}^\alpha(\mathbf{z})).$$

Here, $\mathbf{w}_{j,\text{true}}^\alpha$ and $\mathbf{w}_{j,\text{noise}}^\alpha$ are defined in the last section. They correspond to the backpropagation of pure data and that of the measurement noise. The contribution of $\mathbf{w}_{j,\text{true}}^\alpha$ is exactly the imaging functional with unperturbed data and it is investigated in Proposition 4.2. The contribution of $\mathbf{w}_{j,\text{noise}}^\alpha$ perturbs the true image. For $\mathbf{z}, \mathbf{z}' \in \Omega$, the covariance function of the TD noisy image is given by

$$\begin{aligned} & \text{Cov}(\mathcal{I}_{\text{WF}}[\{\mathbf{U}_j^\alpha\}](\mathbf{z}), \mathcal{I}_{\text{WF}}[\{\mathbf{U}_j^\alpha\}](\mathbf{z}')) \\ &= c_\alpha^2 \frac{1}{n^2} \sum_{j,l=1}^n \mathbb{E}[\Re\{\nabla \mathbf{U}_j^\alpha(\mathbf{z}) : \mathbb{M}'\nabla \mathbf{w}_{j,\text{noise}}^\alpha(\mathbf{z})\} \Re\{\nabla \mathbf{U}_l^\alpha(\mathbf{z}') : \mathbb{M}'\nabla \mathbf{w}_{l,\text{noise}}^\alpha(\mathbf{z}')\}] \\ &= c_\alpha^2 \frac{1}{2n^2} \sum_{j,l=1}^n \Re \mathbb{E}[(\nabla \mathbf{U}_j^\alpha(\mathbf{z}) : \mathbb{M}'\nabla \mathbf{w}_{j,\text{noise}}^\alpha(\mathbf{z}))(\overline{\nabla \mathbf{U}_l^\alpha(\mathbf{z}') : \mathbb{M}'\nabla \mathbf{w}_{l,\text{noise}}^\alpha(\mathbf{z}')})] \\ &= c_\alpha^2 \frac{1}{2n^2} \sum_{j=1}^n \Re \left\{ \nabla \mathbf{U}_j^\alpha(\mathbf{z}) : \mathbb{M}' \left[\mathbb{E}[\nabla \mathbf{w}_{j,\text{noise}}^\alpha(\mathbf{z}) \overline{\nabla \mathbf{w}_{j,\text{noise}}^\alpha(\mathbf{z}')}] : \mathbb{M}' \overline{\nabla \mathbf{U}_j^\alpha(\mathbf{z}')} \right] \right\}. \end{aligned}$$

Using (5.11), we find that

$$\mathbb{E}[\nabla \mathbf{w}_{j,\text{noise}}^\alpha(\mathbf{z}) \overline{\nabla \mathbf{w}_{j,\text{noise}}^\alpha(\mathbf{z}')}] = -\frac{\sigma_{\text{noise}}^2}{4c_\alpha\omega} \Im m \nabla_{\mathbf{z}} \nabla_{\mathbf{z}'} \{\mathbf{\Gamma}_{0,\alpha}^\omega(\mathbf{z} - \mathbf{z}')\}.$$

After substituting this term into the expression of the covariance function, we find that it becomes

$$\frac{c_\alpha \sigma_{\text{noise}}^2}{4\omega} \frac{1}{2n} \sum_{j=1}^n \Re \left\{ \nabla \mathbf{U}_j^\alpha(\mathbf{z}) : \mathbb{M}' \left[\Im m \{\nabla^2 \mathbf{\Gamma}_{0,\alpha}^\omega(\mathbf{z} - \mathbf{z}')\} : \mathbb{M}' \overline{\nabla \mathbf{U}_j^\alpha(\mathbf{z}')} \right] \right\}.$$

The sum has exactly the form that was analyzed in the proof of Proposition 3.4. Using similar techniques, we finally obtain that

$$\text{Cov}(\mathcal{I}_{\text{WF}}[\{\mathbf{U}_j^\alpha\}](\mathbf{z}), \mathcal{I}_{\text{WF}}[\{\mathbf{U}_j^\alpha\}](\mathbf{z}')) = \mu_0 \left(\frac{c_\alpha}{\omega}\right)^3 \left(\frac{\pi}{\kappa_\alpha}\right)^{d-2} \left(\frac{\kappa_S}{\kappa_\alpha}\right)^2 \frac{\sigma_{\text{noise}}^2}{2n} J_{\alpha,\alpha}(\mathbf{z}, \mathbf{z}'), \quad (5.15)$$

where $J_{\alpha,\alpha}$ is defined by (3.24). The variance of the TD image can also be obtained from (5.15). As in the case of density contrast, the typical shape of hot spots in the image corrupted by noise is the same as the main peak of the true image. Further, the effect of measurement noise is reduced by a factor of \sqrt{n} by using n plane waves. In particular, the SNR of the TD image is given by

$$\text{SNR} = \frac{\delta^d \sqrt{\mu_0 \omega}}{\sqrt{c_\alpha^3}} \left(\frac{\pi}{\kappa_\alpha} \right)^{\frac{d-2}{2}} \frac{\kappa_S}{\kappa_\alpha} \frac{4\sqrt{2n}}{\sigma_{\text{noise}}} \sqrt{J_{\alpha,\alpha}(\mathbf{z}_a, \mathbf{z}_a)}. \quad (5.16)$$

6 Statistical stability with medium noise

In the previous section, we demonstrated that the proposed imaging functional using multi-directional plane waves is statistically stable with respect to uncorrelated measurement noises. Now we investigate the case of medium noise, where the constitutional parameters of the elastic medium fluctuate around a constant background.

6.1 Medium noise model

For simplicity, we consider a medium that fluctuates in the density parameter only. That is,

$$\rho(\mathbf{x}) = \rho_0[1 + \gamma(\mathbf{x})], \quad (6.1)$$

where ρ_0 is the constant background and $\rho_0\gamma(\mathbf{x})$ is the random fluctuation in the density. Note that γ is real valued.

Throughout this section, we will call the homogeneous medium with parameters $(\lambda_0, \mu_0, \rho_0)$ the reference medium. The background medium refers to the one without inclusion but with density fluctuation. Consequently, the background Neumann problem of elastic waves is no longer (2.21). Indeed, that equation corresponds to the reference medium and its solution will be denoted by $\mathbf{U}^{(0)}$. The new background solution is

$$\begin{cases} (\mathcal{L}_{\lambda_0, \mu_0} + \rho_0 \omega^2 [1 + \gamma]) \mathbf{U} = 0, & \text{on } \Omega, \\ \frac{\partial \mathbf{U}}{\partial \nu} = \mathbf{g} & \text{on } \partial\Omega, \end{cases} \quad (6.2)$$

Similarly, the Neumann function associated to the problem in the reference medium will be denoted by $\mathbf{N}^{\omega, (0)}$. We denote by \mathbf{N}^ω the Neumann function associated to the background medium, that is,

$$\begin{cases} (\mathcal{L}_{\lambda_0, \mu_0} + \rho_0 \omega^2 [1 + \gamma(\mathbf{x})]) \mathbf{N}^\omega(\mathbf{x}, \mathbf{y}) = -\delta_{\mathbf{y}}(\mathbf{x}) \mathbf{I}_2, & \mathbf{x} \in \Omega, \quad \mathbf{x} \neq \mathbf{y}, \\ \frac{\partial \mathbf{N}^\omega}{\partial \nu}(\mathbf{x}, \mathbf{y}) = 0 & \mathbf{x} \in \partial\Omega. \end{cases} \quad (6.3)$$

We assume that γ has small amplitude so that the Born approximation is valid. In particular, we have

$$\mathbf{N}^\omega(\mathbf{x}, \mathbf{y}) \simeq \mathbf{N}^{\omega, (0)}(\mathbf{x}, \mathbf{y}) + \rho_0 \omega^2 \int_{\Omega} \mathbf{N}^{\omega, (0)}(\mathbf{x}, \mathbf{z}) \gamma(\mathbf{z}) \mathbf{N}^{\omega, (0)}(\mathbf{z}, \mathbf{y}) d\mathbf{y}. \quad (6.4)$$

As a consequence, we also have that $\mathbf{U} \simeq \mathbf{U}^{(0)} - \mathbf{U}^{(1)}$ where

$$\mathbf{U}^{(1)}(\mathbf{x}) = -\rho_0\omega^2 \int_{\Omega} \mathbf{N}^{\omega,(0)}(\mathbf{x}, \mathbf{z})\gamma(\mathbf{z})\mathbf{U}^{(0)}(\mathbf{z})d\mathbf{z}. \quad (6.5)$$

Let σ_γ denotes the typical size of γ , the remainders in the above approximations are of order $o(\sigma_\gamma)$.

6.2 Statistics of the speckle field in the case of a density contrast only

We assume that the inclusion has density contrast only. The backpropagation step constructs \mathbf{w} as follows:

$$\mathbf{w}(\mathbf{x}) = \int_{\partial\Omega} \mathbf{\Gamma}_0^\omega(\mathbf{x}, \mathbf{z}) \overline{\left(\frac{1}{2}I - \mathcal{K}_\Omega^{\omega,(0)}\right)[\mathbf{U}^{(0)} - \mathbf{u}_{\text{meas}}](\mathbf{z})} d\sigma(\mathbf{z}), \quad \mathbf{x} \in \Omega. \quad (6.6)$$

We emphasize that the backpropagation step uses the reference fundamental solutions, and the differential measurement is with respect to the reference solution. These are necessary steps because of the fluctuation in the background medium or equivalently, because of the fact that the background solution is unknown.

Writing the difference between $\mathbf{U}^{(0)}$ and \mathbf{u}_{meas} as the sum of $\mathbf{U}^{(0)} - \mathbf{U}$ and $\mathbf{U} - \mathbf{u}_{\text{meas}}$. These two differences are estimated by $\mathbf{U}^{(1)}$ in (6.5) and by (2.22), respectively. Using Lemma 2.1, we find that

$$\begin{aligned} \mathbf{w}(\mathbf{x}) = & -\rho_0\omega^2 \int_{\partial\Omega} \mathbf{\Gamma}_0^\omega(\mathbf{x} - \mathbf{z}) \int_{\Omega} \overline{\mathbf{\Gamma}_0^\omega(\mathbf{z} - \mathbf{y})\mathbf{U}^{(0)}(\mathbf{y})}\gamma(\mathbf{y})d\mathbf{y}d\sigma(\mathbf{z}) \\ & - C\delta^d \int_{\partial\Omega} \mathbf{\Gamma}_0^\omega(\mathbf{x} - \mathbf{z})\overline{\mathbf{\Gamma}_0^\omega(\mathbf{z} - \mathbf{z}_a)}\mathbf{U}^{(0)}(\mathbf{z}_a)d\sigma(\mathbf{z}) + O(\sigma_\gamma\delta^d) + o(\sigma_\gamma), \quad \mathbf{x} \in \Omega, \end{aligned} \quad (6.7)$$

where $C = \omega^2(\rho_0 - \rho_1)|B|$. The second term is the leading contribution of $\mathbf{U} - \mathbf{u}_{\text{meas}}$ given by approximating the unknown Neumann function and the background solution by those associated to the reference medium. The leading error in this approximation is of order $O(\sigma_\gamma\delta^d)$ and can be written explicitly as

$$\begin{aligned} & C\rho_0\omega^2\delta^d \int_{\partial\Omega} \mathbf{\Gamma}_0^\omega(\mathbf{x}, \mathbf{z}) \int_{\Omega} \overline{\mathbf{\Gamma}_0^\omega(\mathbf{z}, \mathbf{y})\mathbf{N}^{\omega,(0)}(\mathbf{y}, \mathbf{z}_a)}\mathbf{U}^{(0)}(\mathbf{z}_a)\gamma(\mathbf{y})d\mathbf{y}d\sigma(\mathbf{z}) \\ & - C\rho_0\omega^2\delta^d \int_{\partial\Omega} \mathbf{\Gamma}_0^\omega(\mathbf{x}, \mathbf{z})\overline{\mathbf{\Gamma}_0^\omega(\mathbf{z}, \mathbf{z}_a)} \int_{\Omega} \overline{\mathbf{N}^{\omega,(0)}(\mathbf{z}_a, \mathbf{y})}\mathbf{U}^{(0)}(\mathbf{y})\gamma(\mathbf{y})d\mathbf{y}d\sigma(\mathbf{z}), \end{aligned}$$

and is neglected in the sequel.

For the Helmholtz decomposition $\mathbf{w}^\alpha, \alpha \in \{P, S\}$, the first fundamental solution $\mathbf{\Gamma}_0^\omega(\mathbf{x} - \mathbf{z})$ in the expression (6.7) should be changed to $\mathbf{\Gamma}_{0,\alpha}^\omega(\mathbf{x} - \mathbf{z})$. We observe that the second term in (6.7) is exactly (3.10). Therefore, we call this term \mathbf{w}_{true} and refer to the other term in the expression as $\mathbf{w}_{\text{noise}}$. Using the Helmholtz-Kirchhoff identity, we obtain

$$\mathbf{w}_{\text{noise}}^\alpha(\mathbf{x}) \simeq -\frac{\rho_0\omega}{c_\alpha} \int_{\Omega} \gamma(\mathbf{y})\Im\{\mathbf{\Gamma}_{0,\alpha}^\omega(\mathbf{x} - \mathbf{y})\}\overline{\mathbf{U}^{(0)}(\mathbf{y})}d\mathbf{y}, \quad \mathbf{x} \in \Omega. \quad (6.8)$$

We have decomposed the backpropagation \mathbf{w}^α into the “true” $\mathbf{w}_{\text{true}}^\alpha$ which behaves like in reference medium and the error part $\mathbf{w}_{\text{noise}}^\alpha$. In the TD imaging functional using multiple

plane waves with equi-distributed directions, the contribution of $\mathbf{w}_{\text{true}}^\alpha$ is exactly as the one analyzed in Proposition 4.1. The contribution of $\mathbf{w}_{\text{noise}}^\alpha$ is a speckle field.

The covariance function of this speckle field, or equivalently that of the TD image corrupted by noise, is

$$\text{Cov}(\mathcal{I}_{\text{WF}}[\{\mathbf{U}_j^\alpha\}](\mathbf{z}), \mathcal{I}_{\text{WF}}[\{\mathbf{U}_j^\alpha\}](\mathbf{z}')) = C_\alpha^2 \frac{1}{n^2} \sum_{j,l=1}^n \mathbb{E}[\Re\{\mathbf{U}_j^{(0),\alpha}(\mathbf{z}) \cdot \mathbf{w}_{j,\text{noise}}^\alpha(\mathbf{z})\} \Re\{\mathbf{U}_l^{(0),\alpha}(\mathbf{z}') \cdot \mathbf{w}_{l,\text{noise}}^\alpha(\mathbf{z}')\}],$$

for $\mathbf{z}, \mathbf{z}' \in \Omega$, where C_α is defined to be $c_\alpha \omega^2 |B'|(\rho'_1/\rho_0 - 1)$. Here $\mathbf{U}^{(0),\alpha}$ are the reference incoming plane waves (3.14).

Using the expression (6.8), we have

$$\begin{aligned} \frac{1}{n} \sum_{j=1}^n \mathbf{U}_j^\alpha(\mathbf{z}) \cdot \mathbf{w}_{j,\text{noise}}^\alpha(\mathbf{z}) &= -b_\alpha \frac{1}{n} \sum_{j=1}^n \int_{\Omega} \gamma(\mathbf{y}) [\mathbf{U}_j^{(0),\alpha}(\mathbf{z}) \otimes \overline{\mathbf{U}_j^{(0),\alpha}(\mathbf{y})}] : \Im m\{\mathbf{\Gamma}_{0,\alpha}^\omega(\mathbf{z} - \mathbf{y})\} d\mathbf{y} \\ &= -b_\alpha \int_{\Omega} \gamma(\mathbf{y}) \frac{1}{n} \sum_{j=1}^n e^{i\kappa_\alpha(\mathbf{z}-\mathbf{y}) \cdot \mathbf{e}_{\theta_j}} \mathbf{e}_{\theta_j}^\alpha \otimes \mathbf{e}_{\theta_j}^\alpha : \Im m\{\mathbf{\Gamma}_{0,\alpha}^\omega(\mathbf{z} - \mathbf{y})\} d\mathbf{y}. \end{aligned}$$

where $b_\alpha = (\rho_0 \omega)/c_\alpha$. Finally, using (3.18) and (3.19) for $\alpha = P$ and S respectively, we obtain that

$$\frac{1}{n} \sum_{j=1}^n \mathbf{U}_j^{(0),\alpha}(\mathbf{z}) \cdot \mathbf{w}_{j,\text{noise}}^\alpha(\mathbf{z}) = b'_\alpha \int_{\Omega} \gamma(\mathbf{y}) |\Im m\{\mathbf{\Gamma}_{0,\alpha}^\omega(\mathbf{z} - \mathbf{y})\}|^2 d\mathbf{y}. \quad (6.9)$$

Here $b'_\alpha = 4b_\alpha \mu_0 (\frac{\pi}{\kappa_\alpha})^{d-2} (\frac{\kappa_S}{\kappa_\alpha})^2$. Note that the sum above is a real quantity.

The covariance function of the TD image simplifies to

$$C_\alpha^2 b'_\alpha{}^2 \int_{\Omega} \int_{\Omega} C_\gamma(\mathbf{y}, \mathbf{y}') |\Im m\{\mathbf{\Gamma}_{0,\alpha}^\omega(\mathbf{z} - \mathbf{y})\}|^2 |\Im m\{\mathbf{\Gamma}_{0,\alpha}^\omega(\mathbf{z}' - \mathbf{y}')\}|^2 d\mathbf{y} d\mathbf{y}', \quad (6.10)$$

where $C_\gamma(\mathbf{y}, \mathbf{y}') = \mathbb{E}[\gamma(\mathbf{y})\gamma(\mathbf{y}')] is the two-point correlation function of the fluctuations in the density parameter.$

Note that when the medium noise is stationary, *i.e.*, statistically homogeneous, the two-point correlation function becomes $C_\gamma(\mathbf{y} - \mathbf{y}')$; that is, it only depends on the relative position of the two points.

6.3 Statistics of the speckle field in the case of an elasticity contrast

The case of elasticity contrast can be considered similarly. The covariance function of the TD image is

$$c_\alpha^2 \frac{1}{n^2} \sum_{j,l=1}^n \mathbb{E}[\Re\{\nabla \mathbf{U}_j^{(0),\alpha}(\mathbf{z}) : \mathbb{M}' \nabla \mathbf{w}_{j,\text{noise}}^\alpha(\mathbf{z})\} \Re\{\nabla \mathbf{U}_l^{(0),\alpha}(\mathbf{z}') : \mathbb{M}' \nabla \mathbf{w}_{l,\text{noise}}^\alpha(\mathbf{z}')\}].$$

Using the expression of $\mathbf{w}_{\text{noise}}^\alpha$, we have

$$\begin{aligned} \frac{1}{n} \sum_{j=1}^n \nabla \mathbf{U}_j^\alpha(\mathbf{z}) : \mathbb{M}' \nabla \mathbf{w}_{j,\text{noise}}^\alpha(\mathbf{z}) &= -b_\alpha \int_{\Omega} \gamma(\mathbf{y}) \frac{1}{n} \sum_{j=1}^n i\kappa_\alpha e^{i\kappa_\alpha(\mathbf{z}-\mathbf{y}) \cdot \mathbf{e}_{\theta_j}} \\ &\quad \mathbf{e}_{\theta_j} \otimes \mathbf{e}_{\theta_j}^\alpha \otimes \mathbf{e}_{\theta_j}^\alpha : [\mathbb{M}' \Im m\{\nabla_{\mathbf{z}} \mathbf{\Gamma}_{0,\alpha}^\omega(\mathbf{z} - \mathbf{y})\}] d\mathbf{y}. \end{aligned}$$

From (3.18) and (3.19), we see that

$$\frac{1}{n} \sum_{j=1}^n i\kappa_\alpha e^{i\kappa_\alpha \mathbf{x} \cdot \mathbf{e}_{\theta_j}} \mathbf{e}_{\theta_j} \otimes \mathbf{e}_{\theta_j}^\alpha \otimes \mathbf{e}_{\theta_j}^\alpha = -4\mu_0 \left(\frac{\pi}{\kappa_\alpha}\right)^{d-2} \left(\frac{\kappa_S}{\kappa_\alpha}\right)^2 \Im m\{\nabla \mathbf{\Gamma}_{0,\alpha}^\omega(\mathbf{x})\}. \quad (6.11)$$

Using this formula, we get

$$\frac{1}{n} \sum_{j=1}^n \nabla \mathbf{U}_j^\alpha(\mathbf{z}) : \mathbb{M}' \nabla \mathbf{w}_{j,\text{noise}}^\alpha(\mathbf{z}) = b'_\alpha \int_{\Omega} \gamma(\mathbf{y}) Q_\alpha^2[\mathbb{M}'](\mathbf{z} - \mathbf{y}) d\mathbf{y}, \quad (6.12)$$

where $Q^2[\mathbb{M}'](\mathbf{x})$ is a non-negative function defined as

$$Q_\alpha^2[\mathbb{M}](\mathbf{x}) = \Im m\{\nabla \mathbf{\Gamma}_{0,\alpha}^\omega(\mathbf{x})\} : [\mathbb{M} \Im m\{\nabla \mathbf{\Gamma}_{0,\alpha}^\omega(\mathbf{x})\}] = a|\nabla \mathbf{\Gamma}_{0,\alpha}^\omega(\mathbf{x})|^2 + b|\nabla^T \mathbf{\Gamma}_{0,\alpha}^\omega(\mathbf{x})|^2. \quad (6.13)$$

The last equality follows from the expression (2.19) of \mathbb{M} and the fact that $\partial_i(\mathbf{\Gamma}_{0,\alpha}^\omega)_{jk} = \partial_j(\mathbf{\Gamma}_{0,\alpha}^\omega)_{ik}$. Note that (6.12) is again a real quantity.

The covariance function of the TD image simplifies to

$$c_\alpha^2 b'_\alpha{}^2 \int_{\Omega} \int_{\Omega} C_\gamma(\mathbf{y}, \mathbf{y}') Q_\alpha^2[\mathbb{M}'](\mathbf{z} - \mathbf{y}) Q_\alpha^2[\mathbb{M}](\mathbf{z}' - \mathbf{y}') d\mathbf{y} d\mathbf{y}', \quad \mathbf{z}, \mathbf{z}' \in \Omega. \quad (6.14)$$

We observe that the speckle field in the TD image induced by medium noise may have long range or short range correlations according to the correlation structure of the medium noise. In fact, it has the same correlation property as the medium noise. We remark also that the further reduction of the effect of measurement noise with rate $1/\sqrt{2n}$ does not appear in the medium noise case. Hence, TD imaging is less stable with respect to medium noise in that sense.

7 Conclusion

In this paper, we performed an analysis of the topological derivative (TD) based elastic inclusion detection algorithm. We have seen that the standard TD based imaging functional may not attain its maximum at the location of the inclusion. Moreover, we have shown that its resolution does not reach the diffraction limit and identified the responsible terms, that are associated to the coupling of different wave-modes. In order to enhance resolution to its optimum, we cancelled out these coupling terms by means of a Helmholtz decomposition and thereby designing a weighted imaging functional. We proved that the modified functional behaves like the square of the imaginary part of a pressure or a shear Green function, depending upon the choice of the incident wave, and then attains its maximum at the true location of the inclusion with a Rayleigh resolution limit, that is, of the order of half a wavelength. Finally, we have shown that the proposed imaging functionals are very stable with respect to measurement noise and moderately stable with respect to medium noise.

In a forthcoming work, we intend to extend the results of the paper to the localization of the small infinitesimal elastic cracks and to the case of elastostatics. In this regard recent contributions [10, 5, 8] are expected to play a key role.

References

- [1] K. Aki and P. G. Richards, *Quantitative Seismology*, Vol. 1, W. H. Freeman & Co., San Francisco, 1980.
- [2] H. Ammari, *An Introduction to Mathematics of Emerging Biomedical Imaging*, Mathematics & Applications, Vol. 62, Springer-Verlag, Berlin, 2008.
- [3] H. Ammari, E. Bretin, J. Garnier and A. Wahab, Time reversal algorithms in viscoelastic media, *submitted*.
- [4] H. Ammari, P. Calmon and E. Iakovleva, Direct elastic imaging of a small inclusion, *SIAM J. Imag. Sci.* 1:(2008), pp. 169–187.
- [5] H. Ammari, J. Garnier, V. Jugnon and H. Kang, Stability and resolution analysis for a topological derivative based imaging functional, *SIAM J. Control Optim.*, 50(1): (2012), pp. 48–76.
- [6] H. Ammari, L. Guadarrama-Bustos, H. Kang and H. Lee, Transient elasticity imaging and time reversal, *Proc. Royal Soc. Edinburgh: Sect. A Math.*, 141:(2011), pp. 1121–1140.
- [7] H. Ammari and H. Kang, Boundary layer techniques for solving the Helmholtz equation in the presence of small inhomogeneities, *J. Math. Anal. Appl.*, 296(1): (2004), pp. 190–208.
- [8] H. Ammari and H. Kang, *Polarization and Moment Tensors: with Applications to Inverse Problems and Effective Medium Theory*, Applied Mathematics Sciences Series, Vol. 162, Springer-Verlag, New York, 2007.
- [9] H. Ammari and H. Kang, *Reconstruction of Small Inhomogeneities from Boundary Measurements*, Lecture Notes in Mathematics, Vol. 1846, Springer-Verlag, Berlin, 2004.
- [10] H. Ammari, H. Kang, H. Lee and J. Lim, Boundary perturbations due to the presence of small linear cracks in an elastic body, *J. Elasticity*, to appear.
- [11] H. Ammari, H. Kang, G. Nakamura and K. Tanuma, Complete asymptotic expansions of solutions of the system of elastostatics in the presence of inhomogeneities of small diameter, *J. Elasticity*, 67:(2002), pp. 97–129.
- [12] J. C  a, S. Garreau, P. Guillaume and M. Masmoudi, The shape and topological optimization connection, *Comput. Meth. Appl. Mech. Engrg.*, 188:(2001), pp. 703–726.
- [13] N. Dominguez and V. Gibiat, Non-destructive imaging using the time domain topological energy method, *Ultrasonics*, 50:(2010), pp. 172–179.
- [14] N. Dominguez, V. Gibiat and Y. Esquerrea, Time domain topological gradient and time reversal analogy: An inverse method for ultrasonic target detection, *Wave Motion*, 42:(2005), pp. 31–52.
- [15] A. Eschenauer, V. V. Kobelev and A. Schumacher, Bubble method for topology and shape optimization of structures, *Struct. Optim.*, 8:(1994), pp. 42–51.

- [16] G. P. Galdi, *An Introduction to the Mathematical Theory of the Navier-Stokes Equations, Vol. I, Linearized Steady Problems*, Springer-Verlag, New York, 1994.
- [17] B. B. Guzina and M. Bonnet, Topologica derivative for the inverse scattering of elastic waves, *Quart. J. Mech. Appl. Math.*, 57(2):(2004), pp. 161–179.
- [18] B. B. Guzina, I. Chikichev, From imaging to material identification: A generalized concept of topological sensitivity, *J. Mech. Phys. Solids*, 55:(2007), pp. 245–279.
- [19] M. Hintermüller and A. Laurain, Electrical impedance tomography: From topology to shape, *Control Cybernet.*, 37:(2008), pp. 913–933.
- [20] M. Hintermüller, A. Laurain, and A. A. Novotny, Second-order topological expansion for electrical impedance tomography, *Adv. Comput. Math.*, 36(2):(2012), pp. 235–265.
- [21] V. A. Korneev and L. R. Johnson, Scattering of P and S waves by a spherically symmetric inclusion, *Pageoph*, 147 (1996), 675–718.
- [22] V. D. Kupradze, *Potential Methods in the Theory of Elasticity*, Danial Davey & Co., New York, 1965.
- [23] M. Masmoudi, J. Pommier and B. Samet, The topological asymptotic expansion for the Maxwell equations and some applications, *Inverse Problems*, 21:(2005), pp. 547–564.
- [24] J. Sokolowski and A. Zochowski, On the topological derivative in shape optimization, *SIAM J. Control Optim.*, 37:(1999), pp. 1251–1272.
- [25] H. Yuan, B. B. Guzina and R. Sinkus, Application of topological sensitivity towards tissue elasticity imaging using magnetic resonance data, *J. Eng. Mech.*, to appear.